

AUG 4 1958

Copy

3

RM A58E05

NACA RM A58E05



UNCLASSIFIED

NACA

# RESEARCH MEMORANDUM

FLIGHT INVESTIGATION OF THE LOW-SPEED CHARACTERISTICS  
OF A 45° SWEEP-WING FIGHTER-TYPE AIRPLANE  
WITH BLOWING BOUNDARY-LAYER CONTROL  
APPLIED TO THE TRAILING-EDGE FLAPS

By Hervey C. Quigley, Seth B. Anderson,  
and Robert C. Innis

Ames Aeronautical Laboratory  
Moffett Field, Calif.

CLASSIFICATION CHANGED

UNCLASSIFIED

By author  
Date 7/19/64  
954

CLASSIFIED DOCUMENT

This material contains information affecting the National Defense of the United States within the meaning of the espionage laws, Title 18, U.S.C., Secs. 793 and 794, the transmission or revelation of which in any manner to an unauthorized person is prohibited by law.

NATIONAL ADVISORY COMMITTEE  
FOR AERONAUTICS

WASHINGTON  
August 4, 1958

LIBRARY COPY

AUG 4 1958

LANGLEY AERONAUTICAL LABORATORY  
LIBRARY, NACA  
HARTFORD, VIRGINIA

UNCLASSIFIED

NATIONAL ADVISORY COMMITTEE FOR AERONAUTICS

RESEARCH MEMORANDUM

FLIGHT INVESTIGATION OF THE LOW-SPEED CHARACTERISTICS

OF A  $45^\circ$  SWEEP-WING FIGHTER-TYPE AIRPLANE

WITH BLOWING BOUNDARY-LAYER CONTROL

APPLIED TO THE TRAILING-EDGE FLAPS\*

By Hervey C. Quigley, Seth B. Anderson,  
and Robert C. Innis

SUMMARY

A flight investigation has been conducted to determine the low-speed flight characteristics of a  $45^\circ$  swept-wing fighter-type airplane with boundary-layer control on the trailing-edge flaps. The effectiveness of the flap with and without boundary-layer control was determined in conjunction with the standard slatted leading edges, a fixed slat drooped  $19^\circ$ , and the slats locked closed. The study also included low-speed flying qualities and a pilot evaluation of the operational use of the boundary-layer control system in landing approaches. Performance computations were made for take-off, climb, and landing.

The results showed that blowing air over the flap deflected  $45^\circ$  for the landing-approach configuration increased the lift coefficient from 0.71 to 0.87. Maximum lift coefficient was increased from 1.14 to 1.26. Improvements in performance were indicated for landing. Pilots' evaluation showed reductions in average landing approach speeds as much as 14 knots due to boundary-layer control. Improvements were noted in the over-all low-speed flying qualities of the airplane due to boundary-layer control.

INTRODUCTION

The need for improving the low-speed flight characteristics of high-speed airplanes is well known. The NACA for a number of years has made studies of current swept-wing airplanes equipped with boundary-layer control to improve the low-speed lift characteristics. Flight investigations of blowing-type boundary-layer control on the trailing-edge flaps

---

\*Title, Unclassified.

of an F-86 type airplane which has a  $35^\circ$  swept wing and a wing thickness of 10 percent are reported in references 1 and 2. In order to extend the studies to wings of greater sweep and reduced thickness, an investigation was conducted on a modified F-100A airplane with blowing-type boundary-layer control on the trailing-edge flaps.

The investigation consisted of flight tests to determine the effect of boundary-layer control on the low-speed lift and drag characteristics, the low-speed flying qualities, the landing approach characteristics, and the computed take-off and landing performance. The results of this investigation are reported herein.

## NOTATION

b	wing span, ft
BLC	boundary-layer control
$C_D$	drag coefficient, $\frac{D}{qS}$
c.g.	center of gravity
$C_L$	lift coefficient, $\frac{L}{qS}$
$\Delta C_L$	increment of lift due to flaps
$C_{L_{max}}$	maximum lift coefficient
$C_\mu$	momentum coefficient, $\frac{W/g}{qS} V_j$
$C_{1/2}$	number of cycles for oscillation to damp to half amplitude
D	drag, lb
g	acceleration of gravity, $32.2 \text{ ft/sec}^2$
h	nozzle height, in.
L	lift, lb
M.A.C.	mean aerodynamic chord
N	engine speed, percent

p	rolling velocity, radians/sec
P	period, sec
q	free-stream dynamic pressure, lb/ft <sup>2</sup>
S	wing area, sq ft
T	engine thrust
T <sub>1/2</sub>	time for oscillations to damp to half amplitude, sec
V	true airspeed, ft/sec
V <sub>app</sub>	minimum comfortable approach speed, knots
v <sub>e</sub>	equivalent side velocity, $\frac{BV}{57.3} \sqrt{\sigma}$ , ft/sec
V <sub>i</sub>	indicated airspeed, knots
V <sub>j</sub>	velocity of blowing jet assuming isentropic expansion, ft/sec
V <sub>S</sub>	stalling speed, knots
w	weight flow of engine bleed air, lb/sec
W	gross weight
$\alpha$	angle of attack, deg
$\beta$	sideslip angle, deg
$\Delta T$	increment of military thrust available minus thrust required
$\delta$	ratio of total pressure at compressor to standard sea-level pressure
$\delta_a$	aileron deflection, deg
$\delta_f$	flap deflection normal to hinge line, deg
$\delta_t$	horizontal-tail angle, deg
$\theta$	ratio of total temperature at compressor to standard sea-level temperature
$\mu$	friction coefficient

$\rho$	mass density of air, slugs/cu ft
$\sigma$	air density ratio
$\phi$	angle of bank, deg
$\left  \frac{\phi}{v_e} \right $	amplitude ratio of the angle of bank to equivalent side velocity in the oscillatory mode, deg/ft/sec

## EQUIPMENT AND TESTS

### Airplane and Boundary-Layer-Control Flap

Airplane.- A 45° swept-wing fighter-type airplane (modified F-100A) was used for this investigation. A two-view sketch of the airplane is shown in figure 1 and a photograph of the airplane during landing is shown in figure 2. Table I presents the geometric data for the test airplane.

All modifications to the airplane to incorporate the trailing-edge boundary-layer-control flap were designed and constructed by North American Aviation, Inc., under an Air Force Contract.

Trailing-edge flap.- The trailing-edge flap was a plain type with a blowing nozzle on the flap radius. Figure 3 is a photograph of the flap. A cross-sectional sketch of the flap showing the nozzle position is presented in figure 4. The nozzle was continuous across the span of the flap. The nozzle height was nominally 0.035 inch with no pressure in the duct. However, under pressure and elevated temperature the nozzle gap increased appreciably. (At maximum engine speed the mean gap increased to about 0.060 inch.)

Ducting and bleed air.- Air for the boundary-layer control system was bled from the last stage of the high-pressure compressor of the J57-engine. The details of the ducting from the engine bleed ports to the flap nozzle are shown in figure 5. The valve to control the flow of bleed air was located in the ducting between the engine and flaps. The valve gate was positioned by a pneumatic system controlled by a mechanical connection to the flap actuating system, the boundary-layer control shut-off solenoid, or the throttle override solenoid. When the flap deflection was 20° or over, the valve gate was fully open. The valve gate was positioned to an intermediate position by the throttle override solenoid when the throttle was advanced past a throttle setting for about 94.5 percent. The valve gate was fully opened at throttle settings above about 94.5 percent by placing the pilots' throttle override cutout switch to the "off" position.

The weight flow of bleed air extracted from the engine at various engine speeds is shown in figure 6. The thrust loss due to engine bleed air is shown in figure 7. These data were obtained on a thrust stand and include the thrust effects of the blowing nozzle with the flaps deflected  $45^{\circ}$ . The weight flow of bleed air and resulting thrust loss at high engine speeds were greater than design because of the increase in nozzle gap with pressure. Also shown in figures 6 and 7 is the effect of the intermediate valve setting when the throttle override solenoid is actuated. The intermediate valve setting reduced the bleed air extracted at maximum power (95.5-percent engine speed) from the engine by 1.8 pounds per second, thereby making 220 pounds more thrust available for take-off or wave-off than would be available with a fully open valve. The intermediate valve position for full throttle operation was the normal position; the full open valve position at full throttle was used only to obtain high momentum coefficient data.

### Instrumentation and Tests

Instrumentation.- Standard NACA recording instruments were used to record airspeed, altitude, acceleration, angles of attack and sideslip, control positions and forces, airplane angular velocities, and duct pressure and temperatures. Free-stream total and static pressures were taken from an NACA swiveling airspeed head mounted on the end of a boom 11 feet ahead of the nose inlet of the airplane. The angle-of-attack vane and yaw vanes were mounted on the boom 9 feet ahead of the nose inlet. The airplane static pressure was calibrated from 200 to 130 knots by the fly-by method and the data extrapolated to lower speeds. Calibrated pressure probes in the ducts near the flap roots were used for obtaining measurements to compute bleed-air flow and momentum coefficient.

A photo panel was used to record engine speed and tail-pipe temperature, free air temperature, and fuel quantity. Photographs of tufts used for flow visualization on the flap and wing were obtained from an externally mounted camera near the tail and an internally mounted camera aft of the cockpit, respectively (fig. 2).

Tests.- The flight tests were conducted between sea level and 10,000 feet altitude and between 200 knots and minimum flight airspeeds. The take-off wing loading was  $64.4$  pounds per square foot and the landing wing loading was considered to be  $55$  pounds per square foot. The center of gravity varied between  $0.318$  M.A.C. at take-off to  $0.294$  M.A.C. at the landing wing loading.

The majority of the tests were conducted with flaps deflected  $45^{\circ}$ ; tests were also made at flap angles of  $0^{\circ}$ ,  $35^{\circ}$ ,  $40^{\circ}$ , and  $49^{\circ}$ . (Flap construction limited the flap deflection to  $49^{\circ}$ .)

The standard F-100 leading-edge slats which have a deflection of  $15^\circ$  were used for all except two series of tests, one with the slats locked closed and another with the slats deflected  $19^\circ$ . For the  $19^\circ$  slat configuration the slat tracks were removed and the slats were attached to the wing with brackets.

The stalling and landing-approach characteristics of the airplane were determined by evaluation flights by four Ames and two Navy pilots. Field carrier-landing type approaches were used for the landing-approach evaluation and were made with the aid of either a Navy landing signal officer or a mirror landing aid.

## RESULTS AND DISCUSSION

### Lift and Drag Characteristics

#### Effect of boundary-layer control on flap lift and maximum lift.-

The effect of  $45^\circ$  flap deflection with and without boundary-layer control on the trim lift and drag coefficient data are presented in figure 8. These data were obtained with the engine power set for that required for level flight near approach speed. The data show a substantial increase in flap lift increment and a moderate increase in maximum lift coefficient due to boundary-layer control.

The flap lift increments with and without boundary-layer control are shown in figure 9. These data, a cross plot of figure 8, show that the flap lift is doubled at  $\alpha = 12^\circ$  (assumed approach  $\alpha$ ) as a result of boundary-layer control. The flap lift increment with boundary-layer control increases as angle of attack increases up to about  $20^\circ$  angle of attack primarily because of the increase in momentum coefficient as speed is decreased.

The flap lift increment increases linearly with increases in flap deflection for an angle of attack of  $12^\circ$  and with power for approach as shown in figure 10. These data indicate that near theoretical flap lift, as computed from the method of reference 3, was realized up to  $49^\circ$  flap deflection.

With the standard F-100 slatted leading-edge the boundary-layer-control flaps increased  $C_{L_{max}}$  by 0.12 and reduced the angle of attack for  $C_{L_{max}}$  about  $4^\circ$  as shown in figure 8.

Effect of wing leading edge on lift and drag.- To determine the amount of leading-edge stall protection offered by the slats the airplane was flown with the slats locked closed and with slats drooped  $19^\circ$ . Figure 11 presents the lift and drag coefficient data for the configuration

with the slats locked closed. These data show that the flap lift was not affected by the slats but the gain in maximum lift coefficient due to the slats varied with the flap configuration. With boundary-layer control the slats increased maximum lift coefficient 0.31 while without boundary-layer control the improvement was 0.24 and with flaps undeflected only 0.15. These data emphasize the fact that as flap lift is increased the requirements for leading-edge stall protection are increased also.

One flight test was made with the slats fixed at  $19^\circ$  deflection. The lift and drag data for this configuration are presented in figure 12. These data show that the boundary-layer-control flap lift is lower and the drag higher with the  $19^\circ$  slats than with the standard  $15^\circ$  slats. Tuft studies of the air flow over the wing indicated that the air flow behind the slats was rougher with the  $19^\circ$  slats than with the standard slats. The rough flow with the  $19^\circ$  slats was probably caused by the large fixed brackets used to attach the slats to the wing. This rough flow ahead of the flap was believed to be responsible for the decrease in flap lift with boundary-layer control. The highest lift coefficient obtained with the  $19^\circ$  slats was not as high as  $C_{L_{max}}$  with the normal slatted leading edge. However, with the  $19^\circ$  slat configuration the minimum flight speed was limited by instability about all three axes and possibly  $C_{L_{max}}$  was not attained.

The effect of momentum coefficient,  $C_\mu$ , on lift.- The variation of lift coefficient with momentum coefficient is shown in figure 13 for various angles of attack. The data for the basic flap configuration show that there was no rapid change in slope which would indicate a  $C_\mu$  for flow attachment. Tuft studies of the flow over the flap indicated that the areas behind the hinge and actuator cutouts on the flap radius (fig. 3) required a higher  $C_\mu$  value for flow attachment than the rest of the flap. However, for the modified flap (cutouts covered) the tuft studies indicated that the flow over the flap was more uniform. It can be seen from the data in figure 13 that except at the highest  $C_\mu$  values, the  $C_\mu$  for a given  $C_L$  is less with the modified flap configuration than for the basic flap. These data graphically illustrate the need for a smooth flap radius if flow requirements are to be minimized.

Effect of engine speed on lift and momentum coefficient.- Since air flow through the blowing nozzle was determined only by nozzle area and pressure, the momentum of the air as it left the nozzle depended on engine speed and altitude. Figure 14 shows the variation of  $C_\mu$  with engine speed at  $C_L = 1$ . The large increases in  $C_\mu$  with engine speed at the high engine speeds were due to the nozzle area increasing as duct pressure increased as well as to the engine compressor characteristics. The momentum coefficients above an engine speed of 85 percent were higher than would be considered optimum since the change in flap lift with momentum coefficient above a  $C_\mu$  value of 0.008 is small (see fig. 13).



In figure 15 the variation of lift coefficient with percent engine speed is presented for  $12^\circ$  angle of attack. It can be seen from these data that for the range of engine speeds for approach (88 to 92 percent) the lift coefficient varies linearly with engine speed. A reduction of lift with a reduction in engine speed gives the pilot an additional means of controlling the landing touchdown point. Also, a smooth change in lift with engine speeds may be a desired characteristic in the control of the glide path during landing approaches.

### Low-Speed Handling Qualities

The low-speed handling qualities of the airplane were investigated both with and without boundary-layer control and in some instances with flaps retracted. The consensus of the Ames pilots was determined. All the pilots who flew the airplane during this investigation considered the over-all handling qualities improved with the boundary-layer control. The numerical rating system used by the pilots is shown in table II.

Static longitudinal stability.- The stick-fixed and stick-free static longitudinal stability was determined by measuring horizontal-tail angles and stick forces in steady flight. The variations of horizontal-tail angle and stick force with lift coefficient are presented in figure 16. The stick-fixed data show that the stability is positive at the lower  $C_L$  and becomes neutral and negative as  $C_{L_{max}}$  is approached. With boundary-layer control the lift coefficient for neutral stability was increased 0.12. Stick-free stability is similar to stick-fixed stability because control forces are obtained by means of a bungee in the longitudinal control system. Static stability values were not obtained near  $C_{L_{max}}$  because of inability of the pilot to determine the proper control position for trim.

The pilots noted the static longitudinal stability and control in the landing approach speed range to be acceptable but with unpleasant characteristics (numerical rating of 4). The following unpleasant characteristics were noted by the pilots: (1) The response to control seemed sluggish and required large motions; (2) two control inputs were required, one to start pitching motion, another to stop the motion; (3) the pitch-up, although considered mild and controllable, was undesirable because of proximity to maximum lift; and (4) the lack of sufficient nose-up trim with boundary-layer control off was considered unsatisfactory.

Trim changes.- The trim changes accompanying lowering the flaps, and turning on the boundary-layer control at 170 knots while holding altitude constant are noted in the following table:

Initial trim condition		Configuration change		Forces, lb	
$\delta_f$ , deg	Pitch correction	$\delta_f$ , deg	BLC	Peak	Steady
0	On	45	Off	Pull 10	Pull 10
0	On	45	On	Push 16	Pull 8
0	Off	45	Off	Push 18	Push 8
0	Off	45	On	Push 20	Push 18

The airplane was equipped with a pitch corrector which would decrease the tail angle by  $4^\circ$  as the flaps were lowered. With the pitch corrector operating, the trim forces accompanying lowering the flaps with and without boundary-layer control were within the 10-pound limit specified in reference 4. Without the pitch corrector, the trim forces exceeded the 10-pound limit. The pilots found the push forces required to maintain a constant altitude to be abnormal and undesirable when lowering the flaps with boundary-layer control.

Dynamic longitudinal stability.— Figure 17 shows the period and damping of the short-period longitudinal oscillation variation with airspeed. It can be seen that the period increases sharply at the lower airspeed. The airspeed at which the sharp increase in period occurs is about 10 knots lower for boundary-layer control than without. There is little difference in time to damp to half amplitude between boundary-layer control on or off, but with boundary-layer control the cycles to half amplitude are greater. The pilots considered the damping satisfactory and essentially the same with and without boundary-layer control.

Static directional stability and dihedral effect.— The static directional stability and dihedral effect were checked by flying the airplane in steady sideslips. These data (fig. 18) for 145 knots airspeed show the variation of rudder and aileron position and force with sideslip angle. The data indicate that for a given sideslip angle, a lower aileron and a higher rudder deflection are required with than without boundary-layer control. This is consistent with the pilots' report that static directional stability was better with boundary-layer control but the dihedral effect seemed less.

Rolling performance.— The rolling performance was improved appreciably by the application of boundary-layer control to the trailing-edge flap. In figure 19 the rolling performance with and without boundary-layer control on flaps deflected  $45^\circ$  and with flaps retracted is compared. Figure 19(a) shows the variation of  $pb/2V$  with airspeed for about three-quarter and full aileron deflection, and figure 19(b) shows the variation of  $pb/2V$  with aileron deflection at 170 knots. These data

show a 30-percent increase in aileron effectiveness due to boundary-layer control. The pilots' rating of the lateral control was increased from the numerical rating of 3 (satisfactory, but with some mildly unpleasant characteristics) with boundary-layer control off to 2 (good, pleasant to fly) with boundary-layer control.

Adverse yaw.- The adverse yaw due to aileron deflection was determined by deflecting the aileron various amounts in flight and measuring the maximum sideslip angles which developed. Figure 20 shows the variation of sideslip angle with aileron deflection in rolls at approximately 140 knots. The data indicated that the adverse yaw was low with little change due to boundary-layer control.

Lateral oscillatory characteristics.- The period and damping of the lateral-directional oscillations excited by a rudder kick or release from steady sideslip are shown in figure 21. Figure 21(a) shows the period, damping-parameter ( $1/C_{1/2}$ ), and rolling-parameter ( $|\phi|/|v_e|$ ) variation with airspeed. These data indicate that at a constant value of airspeed only small changes in the period occurred as a result of boundary-layer control; however, the damping as measured by  $1/C_{1/2}$  was less with boundary-layer control on. In figure 21(b) the damping parameter,  $1/C_{1/2}$ , variation with rolling parameter,  $|\phi|/|v_e|$ , is shown along with the requirement specified in reference 4. These data show that with boundary-layer control the damping is only slightly above the requirements for airplanes with yaw damper inoperative. (This airplane was not equipped with a yaw damper.) The pilots rated the damping of lateral directional oscillation characteristics acceptable but with unpleasant characteristics (numerical rating of 4).

The pilots' opinions of the changes in the lateral-directional characteristics due to boundary-layer control are summarized as follows: (1) The dihedral effect appeared less; (2) the damping was less but control was better, which makes the airplane easier to fly in rough air. This was perhaps due to the improved aileron effectiveness and better static directional stability.

Stalling characteristics.- The stalling characteristics of the airplane with the standard slats were determined at about 10,000 feet altitude. As minimum flight speed was approached, there was a deterioration in stability about all three axes and an increase in the rate of sink. The airplane did not have a definite stall which was identifiable by the pilots. However, the lift curves (fig. 8) showed a peak which could be considered  $C_{L_{max}}$ . Stalling speeds based on these  $C_{L_{max}}$  values have been computed, assuming thrust required for approach speeds and 22,000 pounds gross weight, and are shown in the following table.

Configuration		$C_{L_{max}}$	Computed stall speed, knots
$\delta_F$ , deg	BLC		
45	On	1.26	108.5
45	Off	1.14	114.5
0	None	1.07	117.5

### Pilots' Evaluation

The landing-approach characteristics of the airplane were evaluated by four NACA and two Naval Air Test Center pilots. The evaluation by the Navy pilots has been reported in reference 5.

Field carrier-landing approaches were used in the landing-approach evaluation. The carrier-type approach was used for this evaluation in order to eliminate as many variables in the approach as possible. Each pilot's evaluation included at least two periods of field carrier landings made with the assistance of either a landing signal officer or a mirror landing aid. From the evaluation, a minimum comfortable approach speed was selected and reasons were determined for not reducing this speed further. The approach speeds are listed in table III, where they are presented both in knots and as a multiple of the computed stalling speed (based on  $C_{L_{max}}$ ). Included for comparison purposes are the results of the two Naval Air Test Center pilots who also flew the airplane (ref. 5). Based on the results of the three pilots who evaluated the airplane with the flaps up, it appears that the flap alone not only reduced the approach speed by 11 to 12 knots, but also reduced the ratio of approach speed to computed stall speed by a decrement of 0.05. With the application of BLC to the flap, each of the pilots was willing to further reduce his approach speed by 7 to 14 knots. Again the speeds chosen represented either the same or a lower percentage of computed stalling speed. Because of the large variance in their choice of approach speeds, the NACA pilots have been divided into two groups in table III. The pilots in group I chose the higher approach speeds and seemed to gain the greatest benefits from BLC, while those in group II were apparently comfortable at lower speeds but had smaller decrements in approach speed when boundary-layer control was applied. Table IV lists the primary and secondary reasons given by the pilots for limiting their approach speeds. The primary reasons are those that basically prevent the pilot from further airspeed reductions, while the secondary reasons are those that may modify slightly his choice of approach speed. The most prevalent reason given for limiting approach speed was the ability to arrest a sink rate, although many other factors seemed to be present. Stability, buffet, and low remaining thrust-to-weight ratio were given as primary influences on the pilots' choice of approach speed. With the application of BLC, all of these were improved with the exception of thrust-to-weight ratio available.

Figure 22 is a plot of lift coefficient versus angle of attack for the three configurations as measured in flight. The lift coefficient corresponding to each pilot's choice of approach speed has been marked on the curves. From this figure it can be seen that the selected approach angle of attack with flaps down was less than with flaps up and the addition of boundary-layer control tended to reduce the selected angle of attack even further. This would account for the comments made by some of the pilots that with the flaps down and BLC on, visibility was improved during the approach. Figure 23 shows the variation of drag with velocity for each configuration and includes a plot of thrust available for both BLC on and off. This plot is of military thrust and does not include afterburning as all of the pilots indicated that they did not like to rely on the use of the afterburner except in an emergency. The difference in thrust is largely attributable to the extraction of engine compressor air for the BLC system. It is of interest to note the position of the pilots' approach speeds in relationship to the minimum drag points. While the minimum drag point moves in a direction consistent with the change in approach speed, little direct correlation between the two is evident. It can be seen that with the application of boundary-layer control to the flap, the curve of drag versus velocity is not only translated to a lower airspeed, but is also rotated. As the airspeed variations associated with changes in angle of attack are directly related to the magnitude of the slopes of these curves, improved speed stability is indicated with BLC.

It was noticed that considerable spread existed in the choice of approach speed between the pilots in groups I and II. In an effort to determine the reasons for this spread, several discussions were held among the evaluating pilots. While there will always be a difference between individuals' choice of what they consider to be a minimum comfortable approach speed, in this case, it was generally concluded that two different techniques or concepts were used. The pilots in group I while using the basic principles of making a precision approach, that is, using throttle to control altitude and longitudinal control to control airspeed, felt that they desired a margin of airspeed which could be used in maneuvering. This margin was such that they could arrest a moderate sink rate or pull-up to gain an arbitrary amount of altitude, add throttle and be able to maintain this altitude. This ability to maneuver was dependent not only on the lift and drag parameters of the airplane, but also upon stability and control characteristics. Such things as lack of trim, poor static longitudinal stability, low damping and sluggish response to controls tend to reduce both the speed and magnitude of the pilots' control motions. This in turn, of course, affects maneuverability. The pilots in group II, on the other hand, relied solely on throttle for altitude control using elevator only to maintain airspeed. Thus, while three of the four pilots gave ability to arrest sink as a primary reason for limiting approach speed, group I pilots were relying more on aerodynamic lift for this, while group II pilots were relying on thrust response and thrust-to-weight ratio available. It should be pointed out

that the pilots in group I by using the latter technique were quite capable of making, and in fact did make, approaches just as slow as those in group II. However, this was below the level of comfort desired. Further examination of the reasons for limiting approach speed revealed one reason why the group II pilots did not gain as much benefit from boundary-layer control as did the group I pilots. The pilots in group I both remarked that with boundary-layer control the thrust available for maneuvering ( $\Delta T/W$ ) was marginal, while both group II pilots considered it unsatisfactory. The reason for this is indicated in figure 23 which shows that with BLC the  $\Delta T/W$  was only about 0.045 at the limiting approach speeds. With BLC off  $\Delta T/W$  was increased to 0.097 which one pilot considered as marginal.

### Performance

Computations were made from measured values of lift, drag, and engine thrust to determine take-off distance, rate of climb, and landing distance. The method outlined in appendix A was used for performance calculation and is considered accurate enough for comparison purposes. The thrust loss due to engine bleed air is considered where applicable.

Take-off distance.- The variations of the computed take-off distances with gross weight are shown in figure 24. It was assumed the attitude at lift-off was limited to  $12^\circ$ . The computations show that with BLC the ground distance was about 5 percent greater than without BLC. The increase in take-off distance was due to the large thrust loss from the use of bleed air for BLC. If the BLC were left off until unstick speed was reached, the take-off distance would be reduced well below that for BLC on for the complete take-off run. The computed total distance over 50 feet is essentially the same for BLC on or off. No attempt was made to determine the optimum flap deflection for take-off.

Rate of climb.- The rate of climb at low airspeeds was greatly reduced by use of BLC, resulting in poor wave-off characteristics. Figure 25 shows the variation of rate of climb at pilots approach speed with gross weight. At landing gross weight the rate of climb is only 900 feet per minute with BLC; however if the bleed air flow were reduced 50 percent at full throttle, this rate of climb would be improved about 300 feet per minute.

Landing distance.- The ground distances required for a landing, with the touchdown attitude assumed limited to  $12^\circ$ , are shown in figure 26. These data which show the variation of landing distance with gross weight indicate that the ground distance would be decreased about 16 percent by use of BLC.

## CONCLUSIONS

The following conclusions can be made from this investigation of blowing boundary-layer control on the trailing-edge flaps of an F-100A airplane.

1. In the landing-approach configuration boundary-layer control on the flaps increased the flap lift increment by 100 percent ( $\alpha = 12^\circ$ ) and  $C_{L_{max}}$  by 0.12 and decreased the angle of attack for  $C_{L_{max}}$  by  $4.5^\circ$ .
2. Boundary-layer control on the flap increased the lift coefficient for neutral longitudinal stability by 0.12.
3. The rate of roll for large aileron deflections at 170 knots airspeed was increased 30 percent as a result of boundary-layer control on the flaps.
4. Boundary-layer control reduced the pilot's minimum comfortable approach speed in field carrier landings by 7 to 14 knots. The amount of this reduction was dependent upon the technique the pilot used in maneuvering during the approach. The minimum comfortable approach speed was limited primarily by the ability to arrest a sink rate.
5. The wave-off characteristics of the airplane were considered by the pilots to be unsatisfactory with boundary-layer control operative because of the low value of the ratio of the engine thrust available (without afterburner) to airplane gross weight.
6. The computed ground roll in landing was 16 percent less with boundary-layer control than without. The computed ground distance for take-off was 5 percent more with boundary-layer control on the flaps deflected  $45^\circ$  than without boundary-layer control, and the computed total distance over 50 feet was essentially the same.

Ames Aeronautical Laboratory  
National Advisory Committee for Aeronautics  
Moffett Field, Calif., May 5, 1958

## APPENDIX

## METHOD USED FOR PERFORMANCE EVALUATION

The following equations and assumptions were used in computing take-off distance, rate of climb, and landing distance.

Take-off distance:

$$\text{Ground run} = \frac{30 W/S}{\sigma(C_{Dg} - \mu C_{Lg})} \log_{10} \left[ \frac{T/W - \mu}{(T/W - \mu) - \frac{C_{Dg} - \mu C_{Lg}}{C_{LT_0}}} \right], \text{ ft}$$

(ref. 6, p. 2).

$$\text{Air distance} = \frac{50 W}{T - D} + \frac{V_{T_0}^2}{g \sqrt{2}}, \text{ ft}$$

(ref. 7, p. 51) where

$C_{Dg}$  = drag coefficient during ground run ( $\alpha = 4^\circ$ )

$C_{Lg}$  = lift coefficient during ground run ( $\alpha = 4^\circ$ )

$C_{LT_0}$  = lift coefficient at  $V_{T_0}$  ( $\alpha = 12^\circ$ )

$D$  = drag at  $V_{T_0}$

$$V_{T_0} = \sqrt{\frac{843(W - T \sin \alpha)}{SC_{LT_0}}}$$

$T$  = take-off thrust (with afterburner)

$\mu = 0.02$

$\sigma$  = ratio of density to sea-level value



Rate of climb:

$$\text{Rate of climb} = 60 V_c \frac{(T - D)}{W}, \text{ ft/min}$$

where

$V_c$  = approach velocity, ft/sec

$T$  = take-off thrust (with afterburner)

$D$  = drag at  $V_c$

Landing distance:

$$\text{Ground run} = \frac{30 W/S}{-\sigma(C_{Dg} - \mu C_{Lg})} \log_{10} \left[ \frac{\mu - T_0/W}{(\mu - T_0/W) + \frac{C_{Dg} - \mu C_{Lg}}{C_{LTD}}} \right], \text{ ft}$$

(ref. 6, p. 2) where

$C_{Dg}$  = drag coefficient during ground run ( $\alpha = 4^\circ$ )

$C_{Lg}$  = lift coefficient during ground run ( $\alpha = 4^\circ$ )

$C_{LTD}$  = lift coefficient at touchdown ( $\alpha = 12^\circ$ )

$\mu = 0.4$

$T_0$  = thrust at idle engine speed

## REFERENCES

1. Anderson, Seth B., Quigley, Hervey C., and Innis, Robert C.: Flight Measurements of the Low-Speed Characteristics of a  $35^{\circ}$  Swept-Wing Airplane With Blowing-Type Boundary-Layer Control on the Trailing-Edge Flaps. NACA RM A56G30, 1956.
2. Quigley, Hervey C., Hom, Francis W. K., and Innis, Robert C.: A Flight Investigation of Area-Suction and Blowing Boundary-Layer Control on the Trailing-Edge Flaps of a  $35^{\circ}$  Swept-Wing Carrier-Type Airplane. NACA RM A57B14, 1957.
3. DeYoung, John: Theoretical Symmetrical Span Loading Due to Flap Deflection for Wings of Arbitrary Plan Form at Subsonic Speeds. NACA Rep. 1071, 1952.
4. Anon.: Military Specification. Flying Qualities of Piloted Airplanes. MIL-F-8785 (ASG) Sept. 1, 1954.
5. Heyworth, L., Jr., and Hancock, V. R.: Navy Evaluation of the Model F-100A Airplane with Boundary Layer Control System. Rep. no. 1, Final Report, Project TED No. PTR AC-29007, Naval Air Test Center, Patuxent River, Md., June 6, 1957.
- ✓ 6. Kettle, D. J.: Ground Performance at Take-Off and Landing. Aircraft Engineering, vol. XXX, no. 347, Jan. 1958, p. 2.
7. Lush, Kenneth J.: Standardization of Take-Off Performance Measurements for Airplanes. TNR-12, Air Force Flight Test Center, Edwards Air Force Base, Calif., 1954.

TABLE I.- GEOMETRIC DATA OF AIRPLANE

<b>Wing</b>	
Airfoil section . . . . .	NACA 64A007
Total area, sq ft . . . . .	400.2
Span, ft . . . . .	38.8
Mean aerodynamic chord, ft . . . . .	11.2
Taper ratio . . . . .	0.26
Aspect ratio . . . . .	3.72
Sweep at 0.25 chord line, deg . . . . .	45
Incidence . . . . .	0
Dihedral . . . . .	0
<b>Aileron</b>	
Area, sq ft . . . . .	37.0
Travel, deg . . . . .	±15
<b>Leading-edge slat</b>	
Span, ft . . . . .	12.7
Span location, inboard end, percent b/2 . . . . .	23.3
Span location, outboard end, percent b/2 . . . . .	89.2
Chord (streamwise), percent wing chord . . . . .	20.0
Rotation, maximum, deg . . . . .	15
<b>Flap</b>	
Area, sq ft . . . . .	29.8
Chord, percent wing chord, average . . . . .	25.0
<b>Horizontal tail</b>	
Airfoil section . . . . .	NACA 65A003.5
Total area, sq ft . . . . .	98.9
Span, ft . . . . .	18.7
Sweep at 0.25 chord line, deg . . . . .	45
<b>Travel</b>	
Leading edge up, deg . . . . .	10
Leading edge down, deg . . . . .	20.6
<b>Vertical tail</b>	
Airfoil section . . . . .	NACA 65A003.5
Total area, sq ft . . . . .	45.2
Total area, rudder, sq ft . . . . .	6.3
Span, ft . . . . .	7.9
Sweep, deg . . . . .	45

TABLE II.- PILOT OPINION RATING SYSTEM

	Adjective rating	Numerical rating	Description	Primary mission accomplished	Can be landed
Normal operation	Satisfactory	1	Excellent, includes optimum	Yes	Yes
		2	Good, pleasant to fly	Yes	Yes
		3	Satisfactory, but with some mildly unpleasant characteristics	Yes	Yes
Emergency operation	Unsatisfactory	4	Acceptable, but with unpleasant characteristics	Yes	Yes
		5	Unacceptable for normal operation	Doubtful	Yes
		6	Acceptable for emergency condition only <sup>1</sup>	Doubtful	Yes
No operation	Unacceptable	7	Unacceptable even for emergency condition <sup>1</sup>	No	Doubtful
		8	Unacceptable - dangerous	No	No
		9	Unacceptable - uncontrollable	No	No

<sup>1</sup>Failure of a stability augments.

TABLE III.- MINIMUM COMFORTABLE APPROACH SPEEDS

20

Group	Pilot	Flaps up	Flaps down - BLC off	Flaps down - BLC on	$\Delta V$ Due flaps	$\Delta V$ Due BLC
I	A	161 (1.37)	149 (1.30)	135 (1.24)	12	14
	B	160 (1.36)	149 (1.30)	136-1/2 (1.26)	11	12-1/2
II	C	149 (1.27)	137-1/2 (1.20)	130 (1.20)	11-1/2	7-1/2
	D	Not evaluated	142 (1.24)	132-1/2 (1.22)	---	9-1/2
Navy pilots	E	Not evaluated	147 (1.28)	137 (1.26)	---	10
	F	Not evaluated	142 (1.24)	134-1/2 (1.24)	---	7-1/2
Spread		12	12-1/2	7		
$V_S$ (computed from $C_{L_{max}}$ )		117.5	114.5	108.5	3	6

Open figures are calibrated airspeed in knots.

Figures in parentheses are ratio of approach speed to computed stall speed ( $V_{app}/V_S$ ).

NACA RM A58E05

TABLE IV.- REASONS FOR LIMITING APPROACH SPEEDS

Group	Pilot	Flaps up	Flaps down - ELC off	Flaps down - ELC on	Pilot control technique
I	A	Primary: ability to arrest sink plus lateral stability and control.	Primary: ability to arrest sink plus $\Delta T/W$ low. Secondary: poor lateral stability and control. Lack of longitudinal trim, uncomfortable stick position. Buffet objectionable. Attitude and visibility marginal.	Primary: ability to arrest sink plus $\Delta T/W$ low.	V <sub>app</sub> determined primarily by aerodynamic ability to arrest sink. Thrust secondary.
	B	Primary: ability to arrest sink. Secondary: directional stability, visibility, and longitudinal stability are objectionable.	Primary: ability to arrest sink. Secondary: buffet, lateral-directional stability, lack of trim, longitudinal stability and control objectionable.	Primary: ability to arrest sink ( $\Delta T/W$ poor).	
II	C	Primary: ability to arrest sink. Secondary: visibility marginal.	Primary: ability to arrest sink. Secondary: visibility marginal plus lack of trim and rearward stick position.	Primary: ability to arrest sink. Secondary: visibility marginal ( $\Delta T/W$ unacceptable).	V <sub>app</sub> determined primarily by $\Delta T/W$ . Aerodynamic control secondary.
	D	Not evaluated.	Primary: buffet. Secondary: poor control power about all axis and visibility.	Primary: $\Delta T/W$ too low. Secondary: longitudinal control power.	
Navy pilots	E	Not evaluated.	Primary: high minimum trim speeds mask other factors.	Primary: Low $\Delta T/W$ .	
	F	Not evaluated.	Primary: lateral and directional stability. Secondary: Lack of speed stability.	Primary: ability to arrest sink.	

[REDACTED]

[REDACTED]

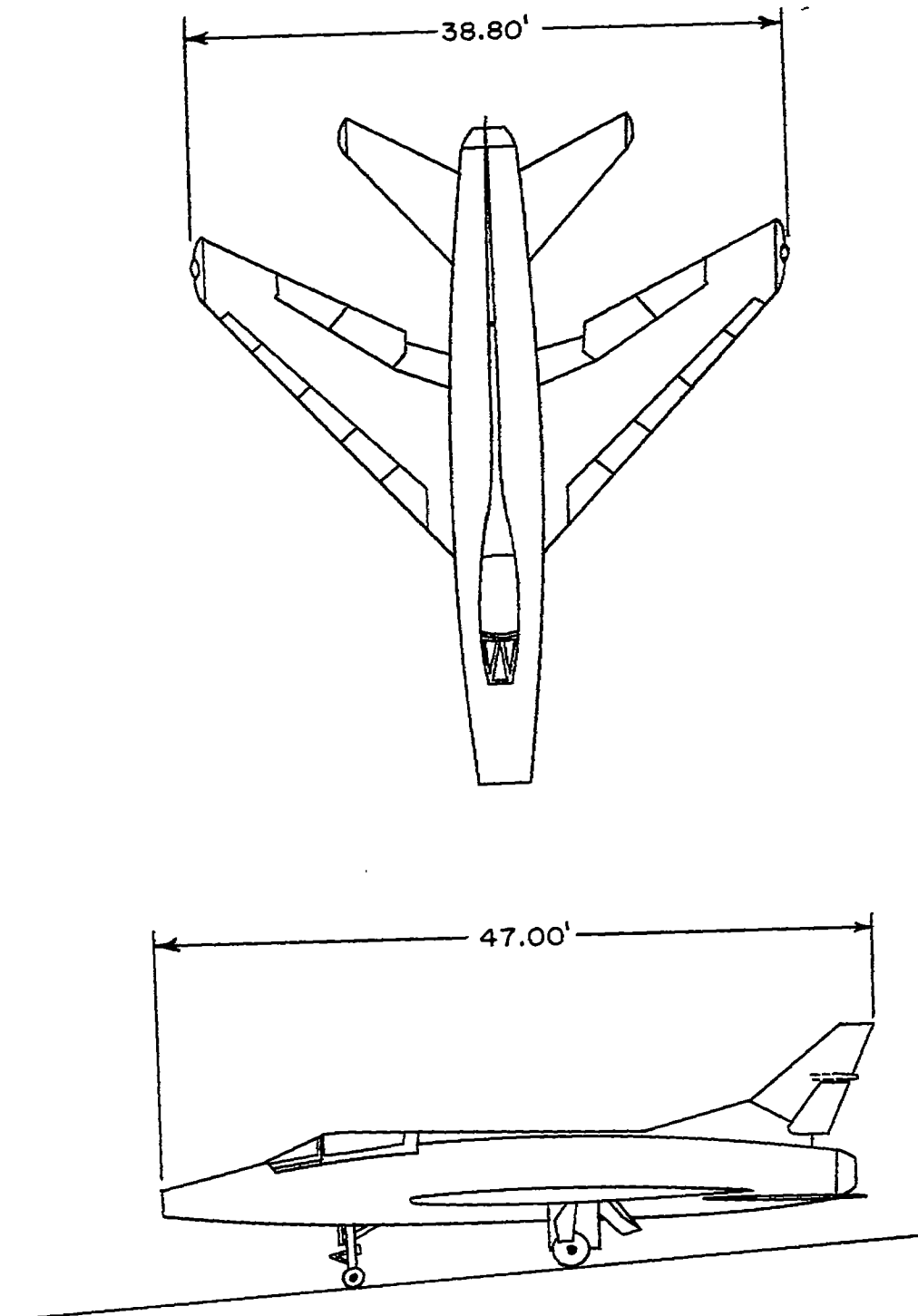
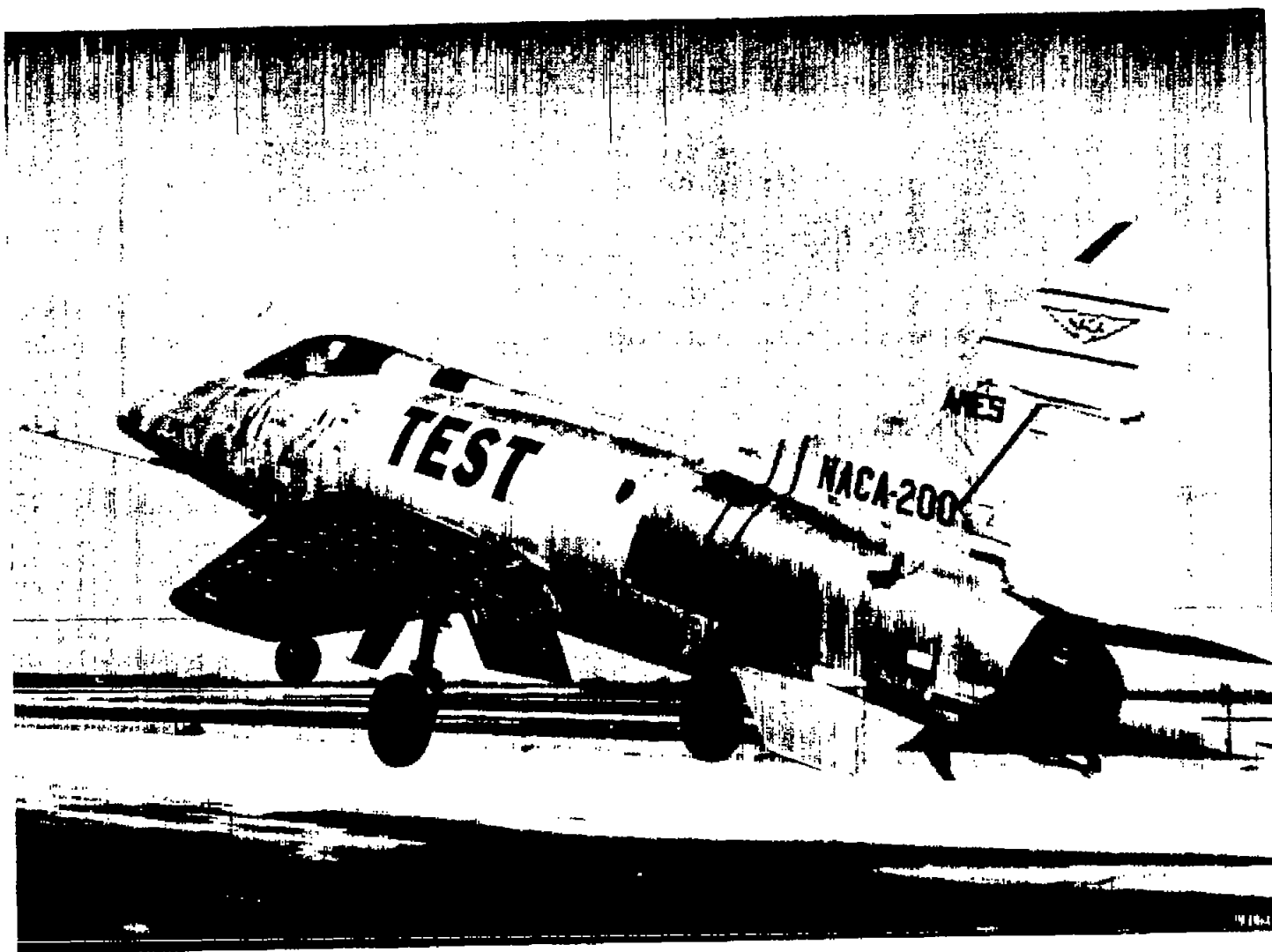


Figure 1.- Two-view drawing of test airplane.





A-22839

Figure 2.- Photograph of test airplane.

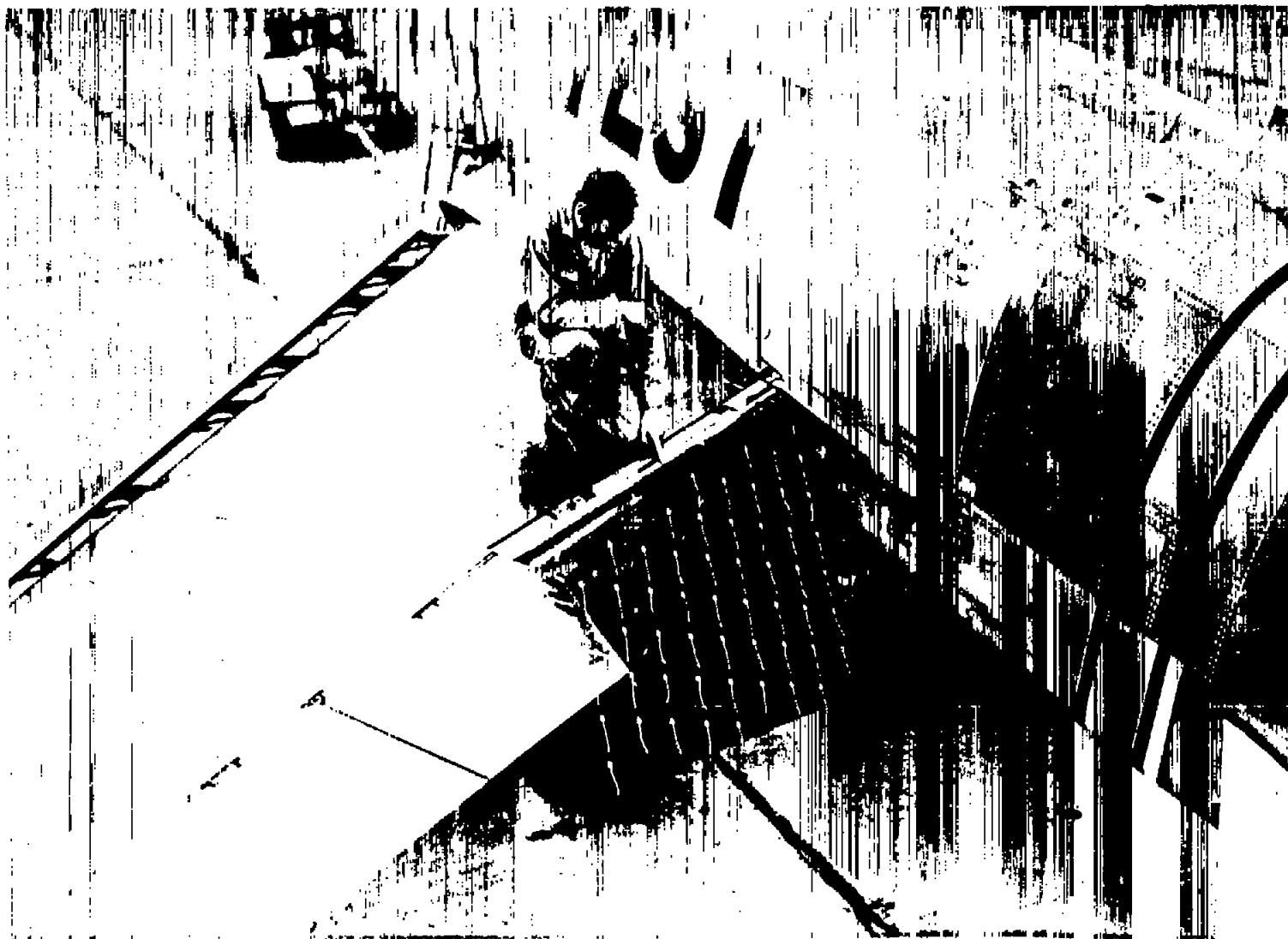


Figure 3.- Photograph of trailing-edge boundary-layer control flap.

A-22511

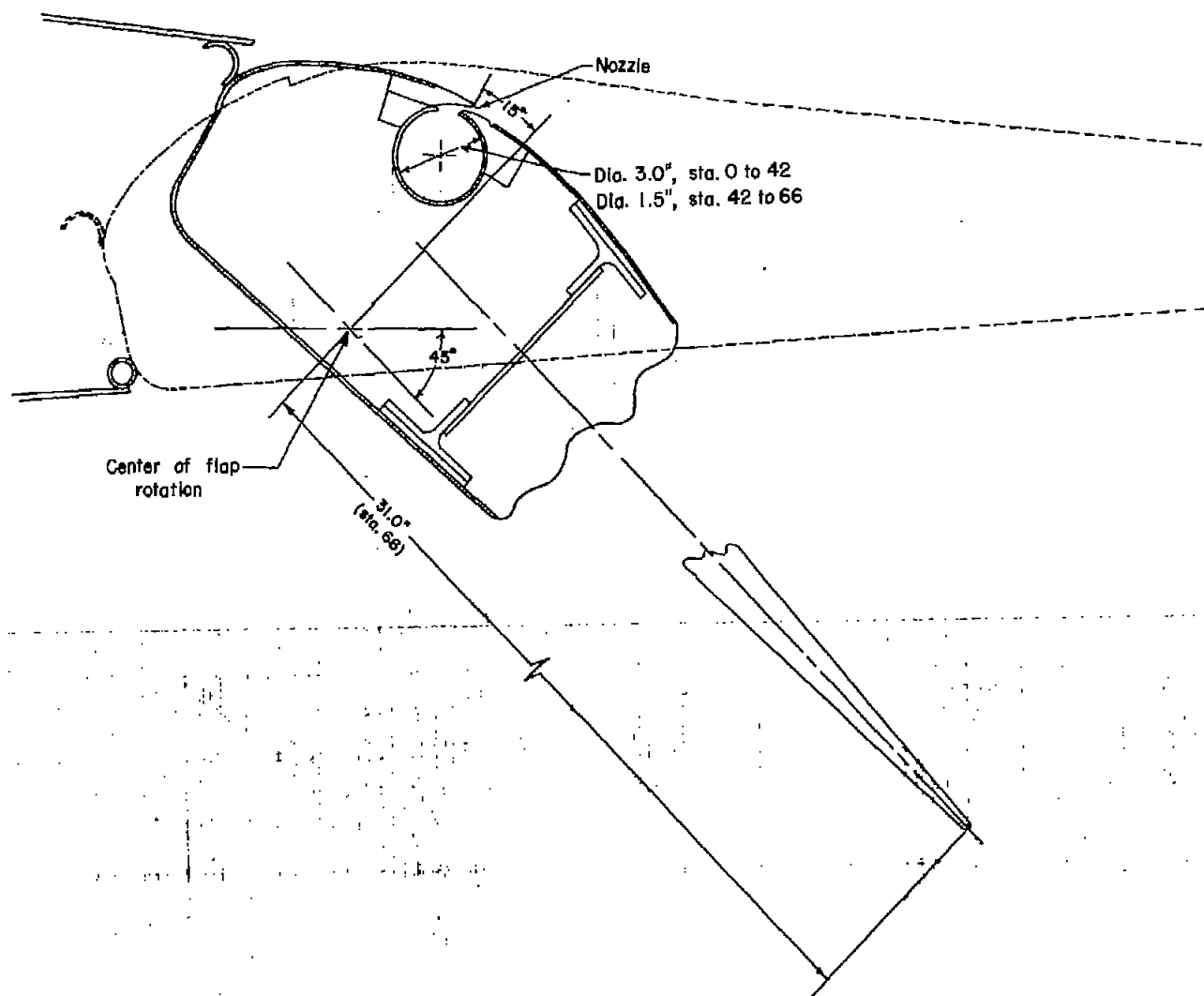


Figure 4.- Cross section of blowing-type flap.

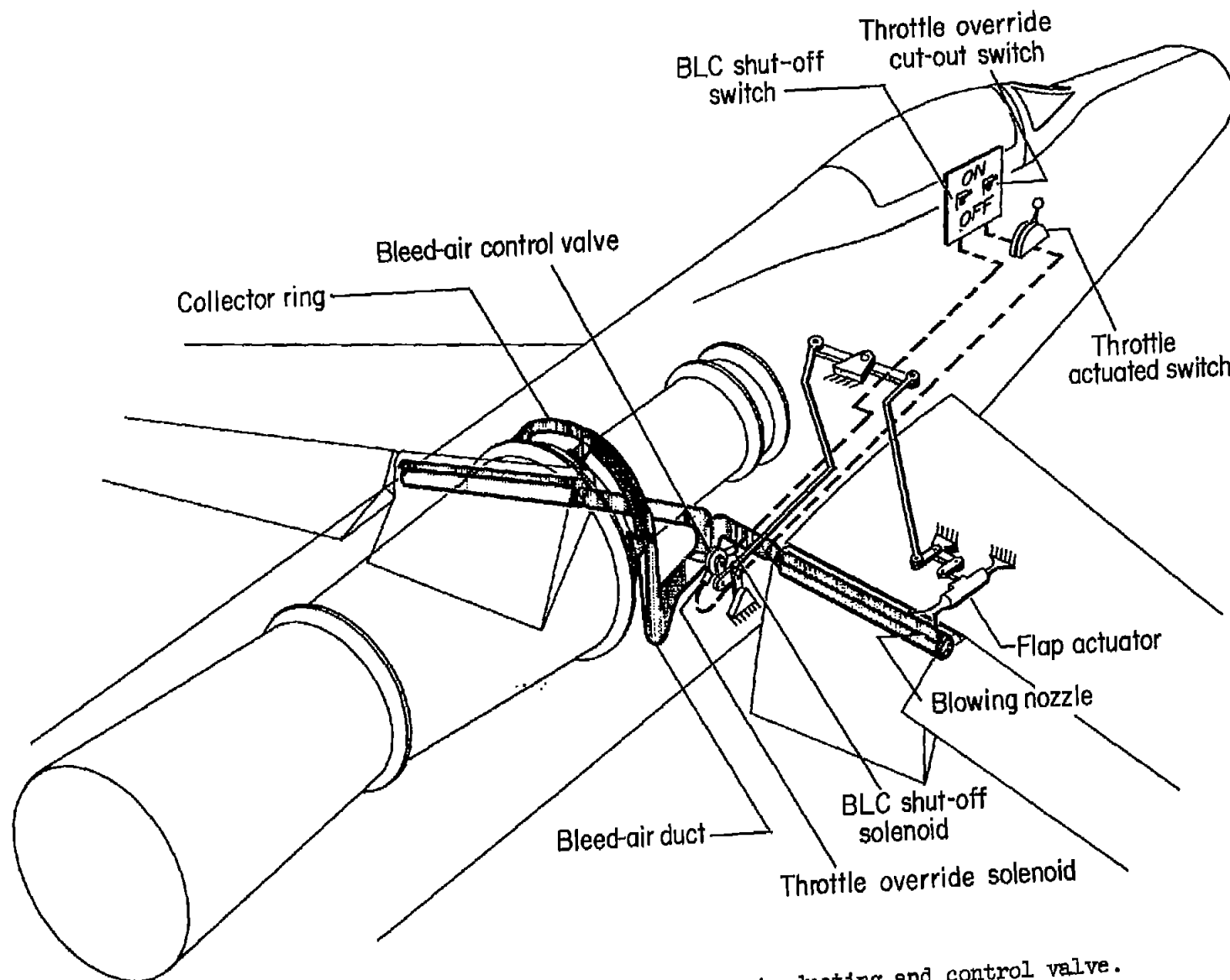


Figure 5.- Schematic drawing of bleed-air ducting and control valve.

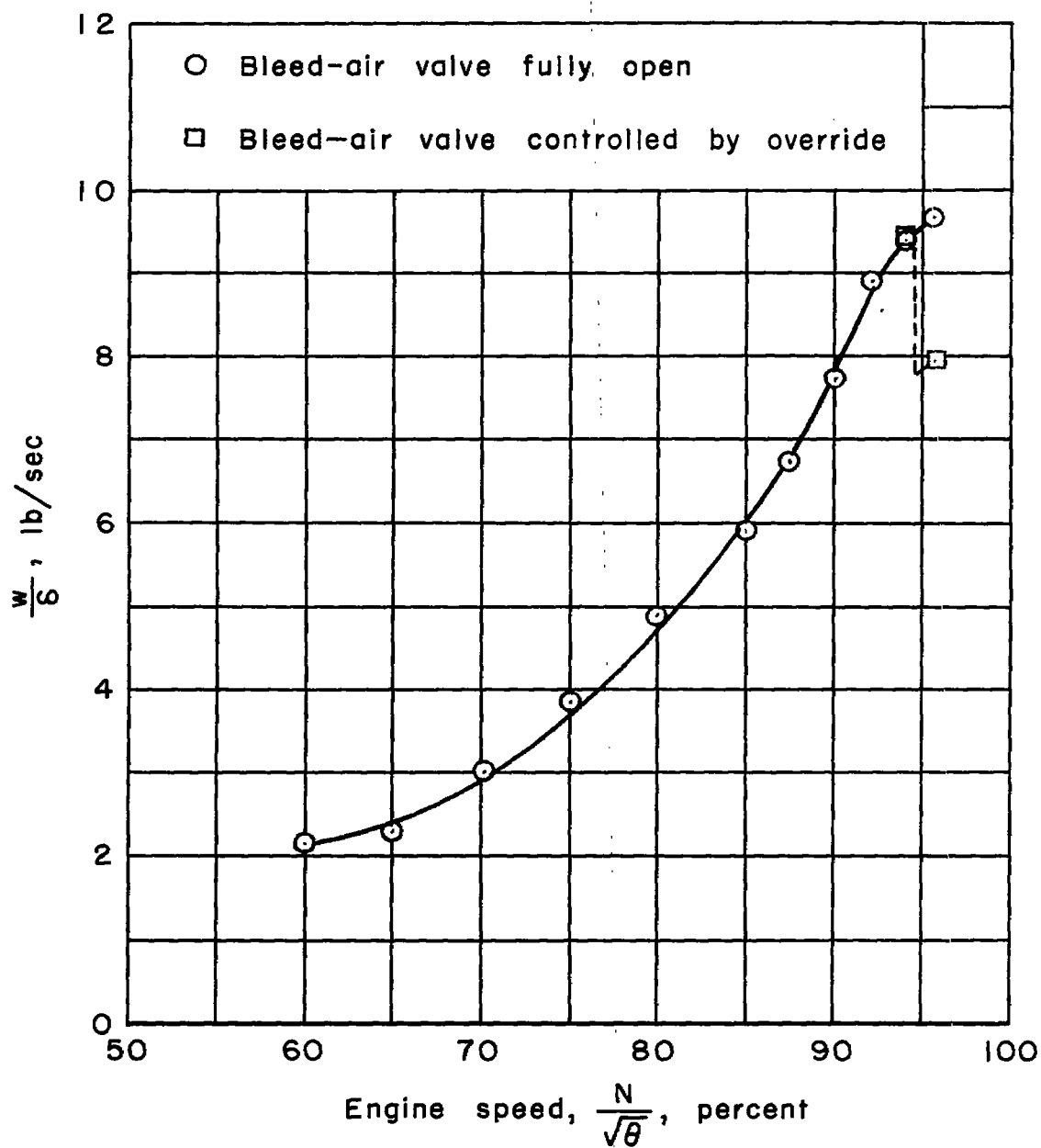


Figure 6.- Variation of weight flow of bleed air with engine speed.

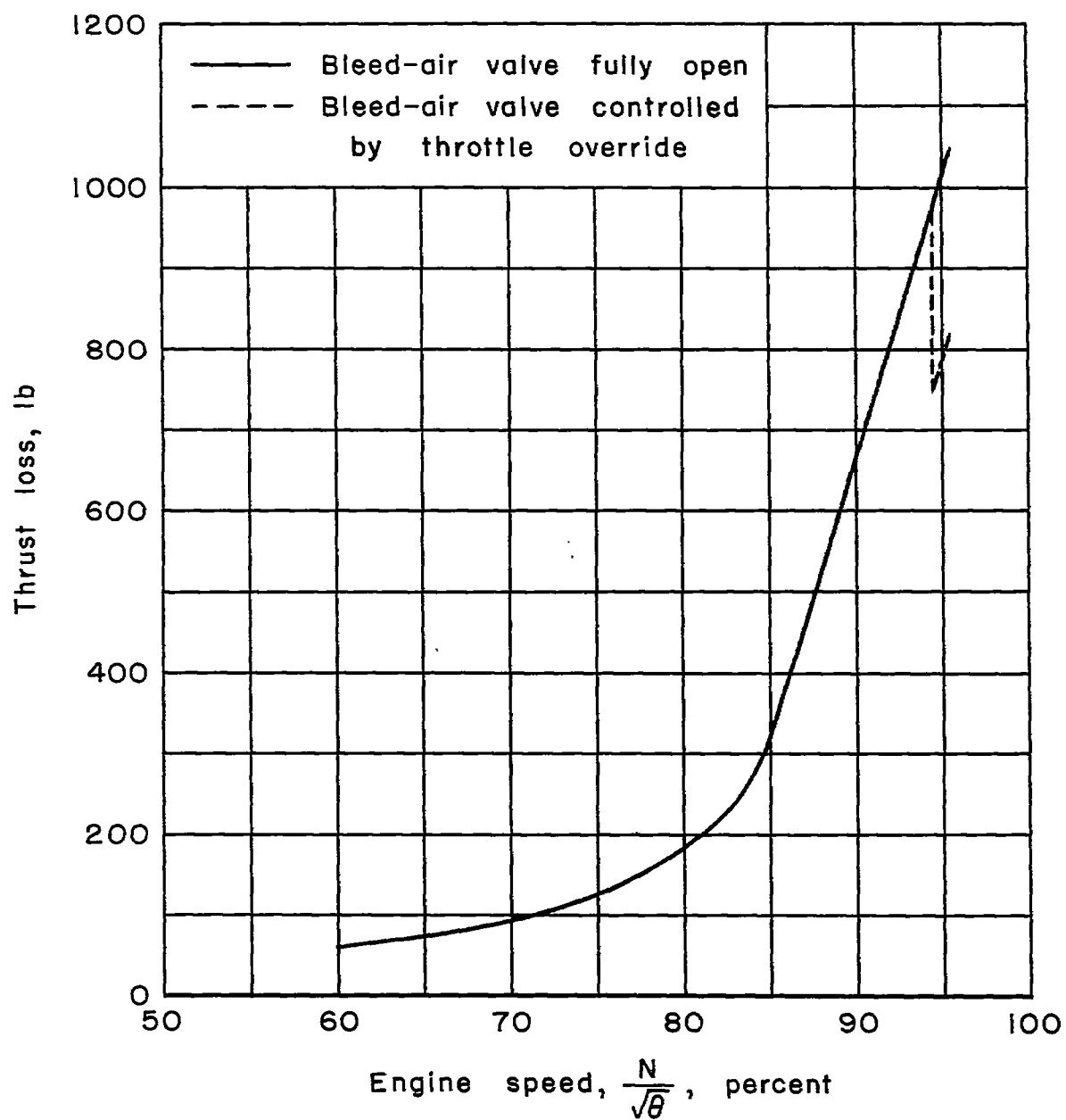


Figure 7.- Variation of engine static-thrust loss due to bleed air with engine speed.

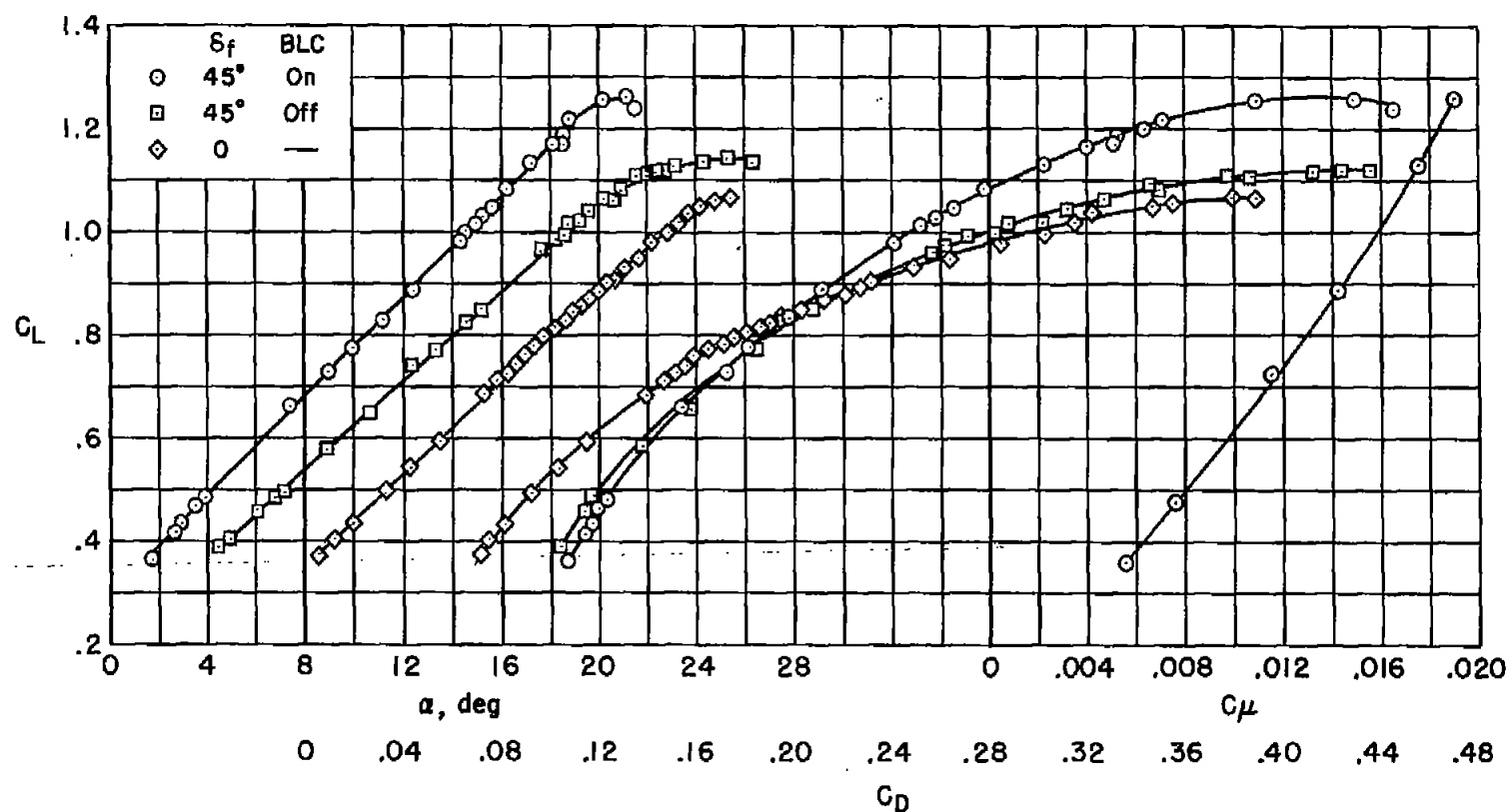


Figure 8.- Lift, drag, and momentum coefficient curves; center of gravity at 0.031 M.A.C.; landing gear down.

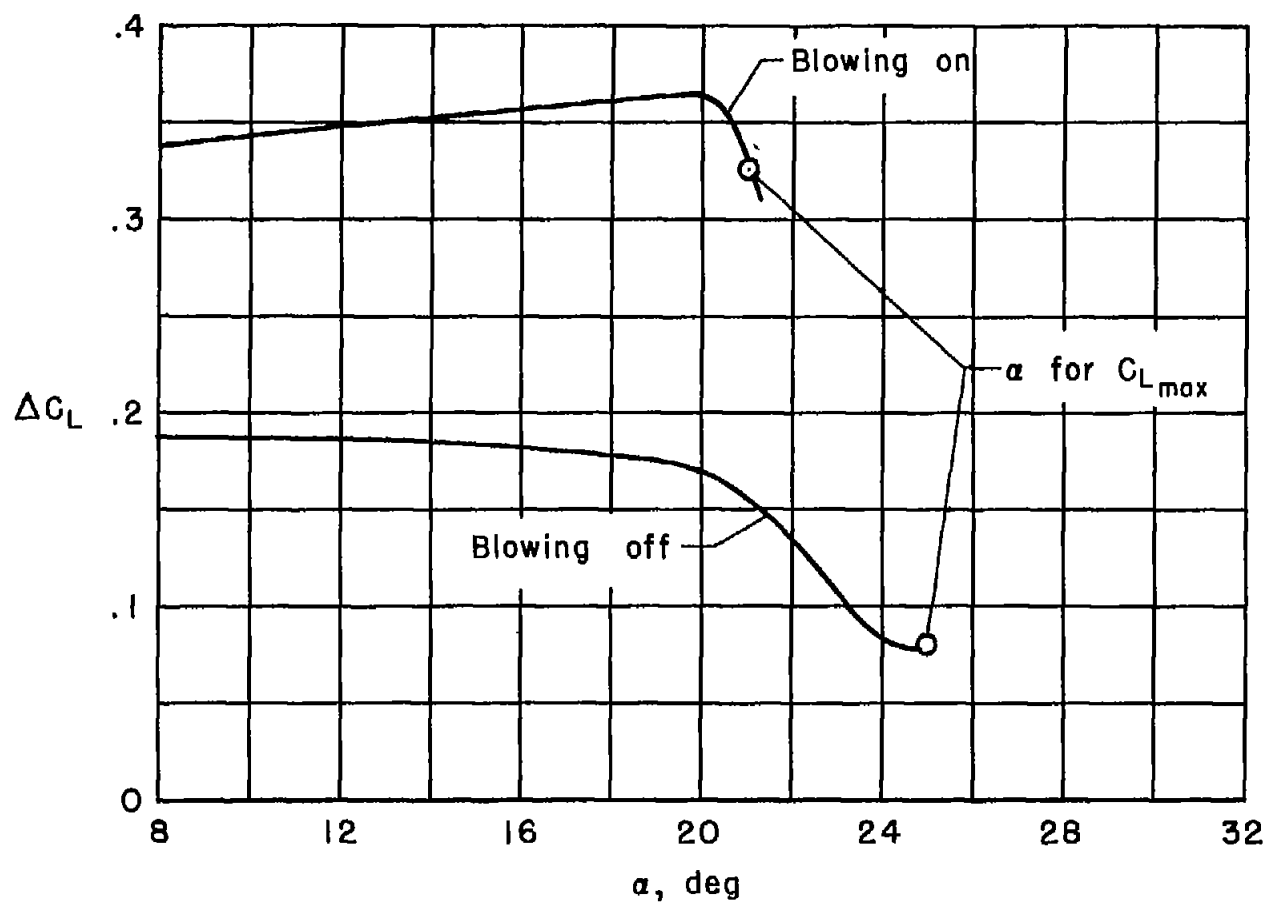


Figure 9.- Variation of flap lift increment with angle of attack;  $\delta_F = 45^\circ$ ; engine speed = 92 percent.



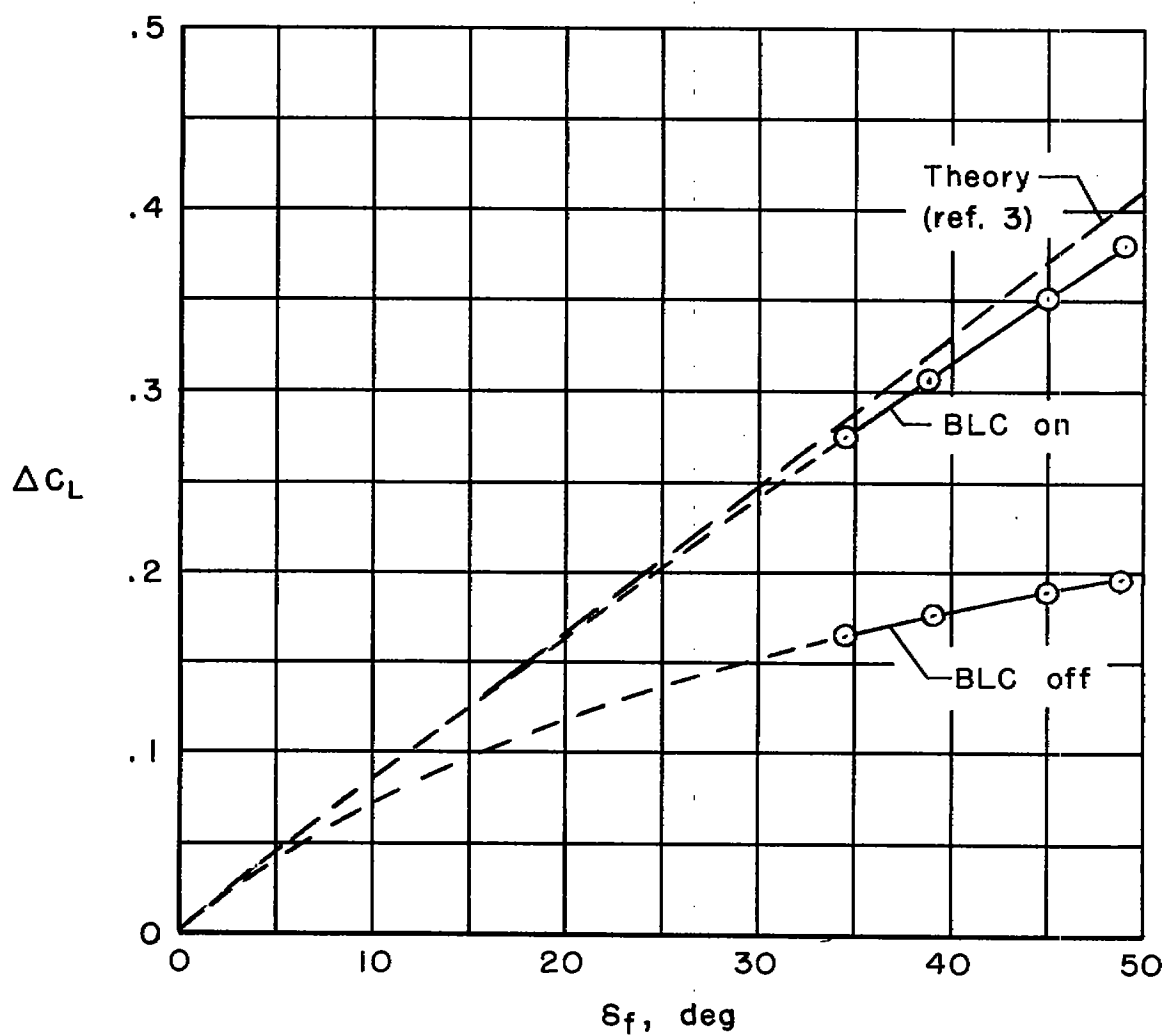


Figure 10.- Variation of flap lift increment with flap angle;  $\alpha = 12^\circ$ ; engine speed = 92 percent.

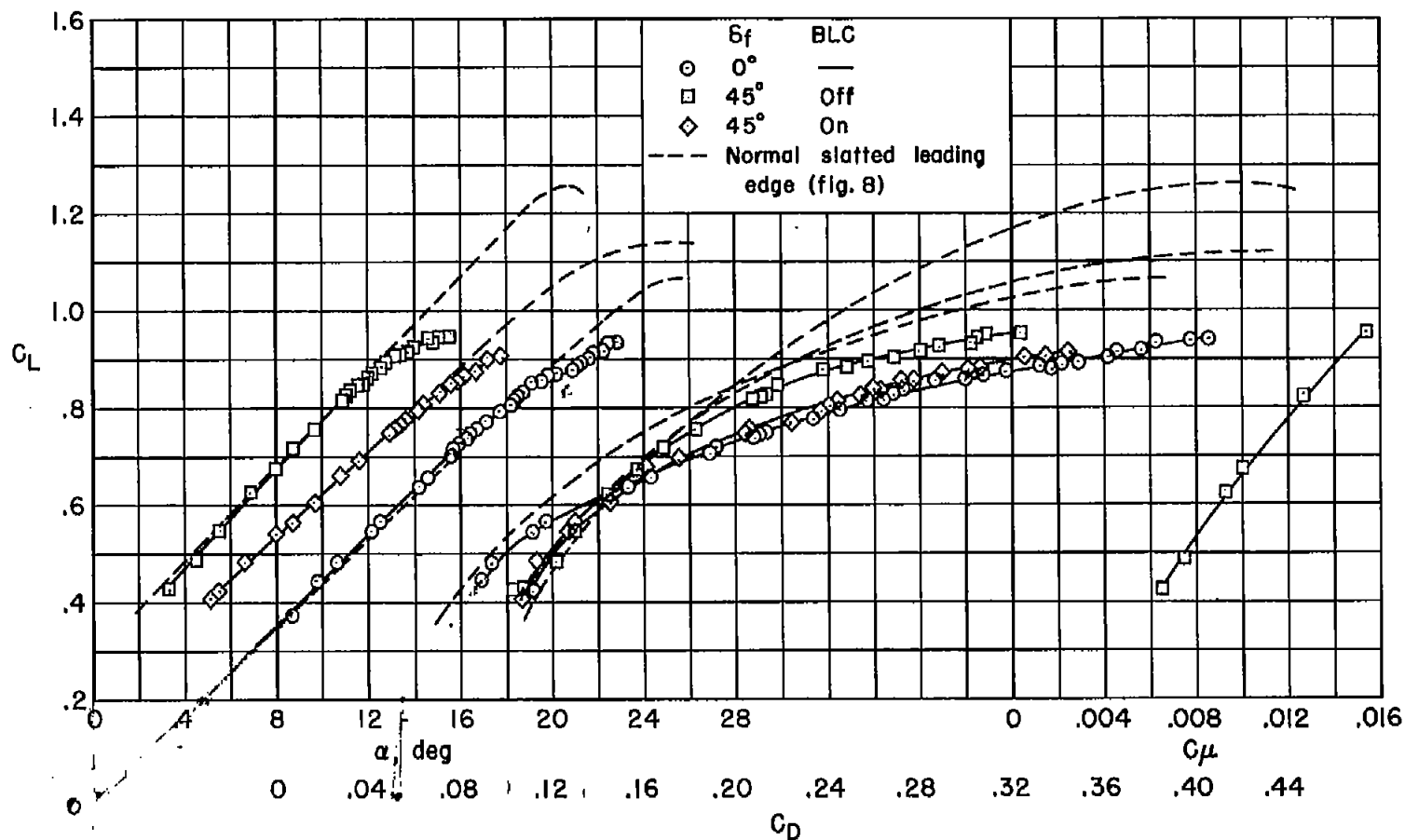


Figure 11.- Lift and drag characteristics with leading-edge slats locked closed; engine speed = 92 percent; center of gravity at 0.31 M.A.C.

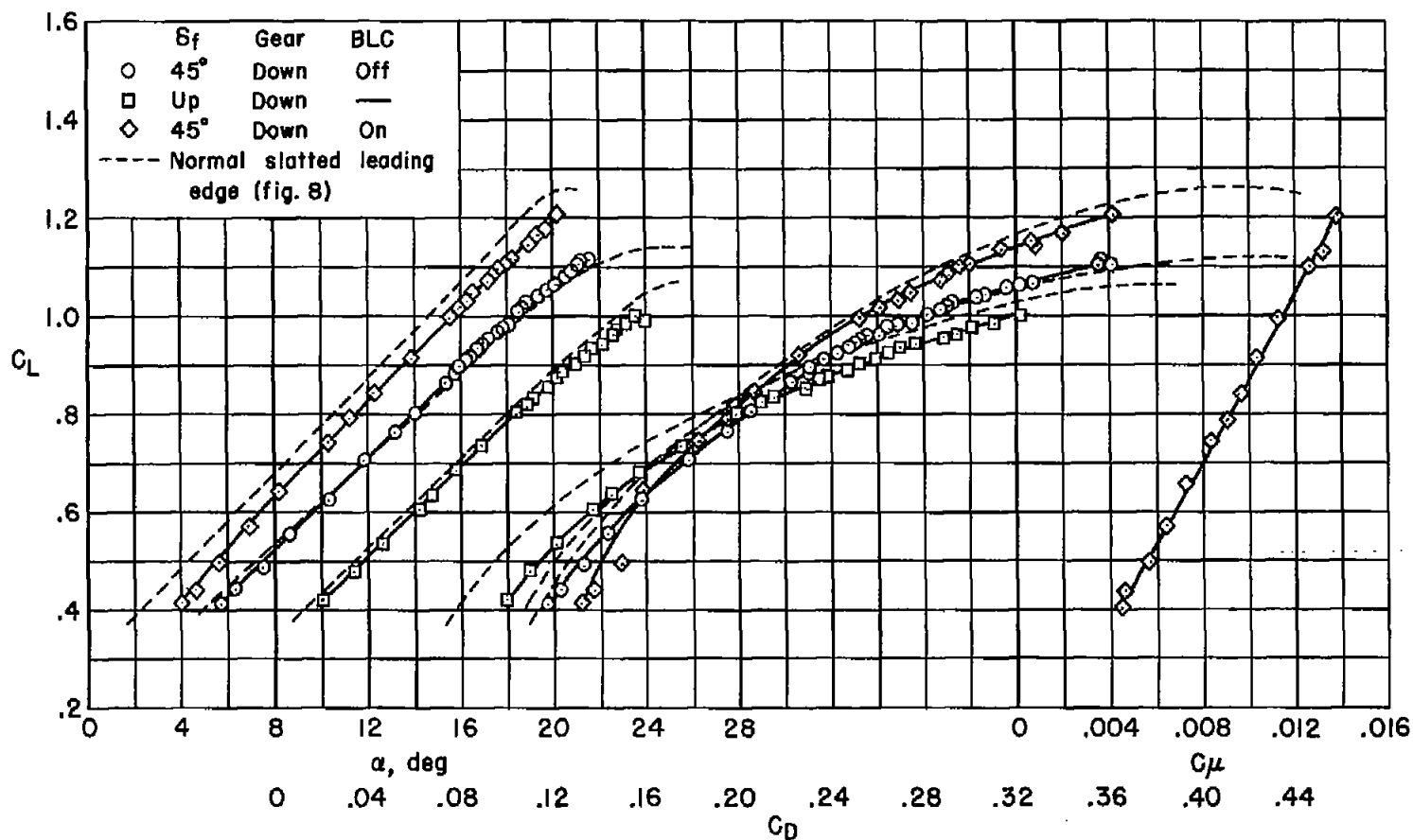


Figure 12.- Lift and drag characteristics with leading-edge slats drooped  $19^\circ$ ;  $\delta_f = 45^\circ$ ; engine speed = 92 percent; center of gravity at 0.31 M.A.C.

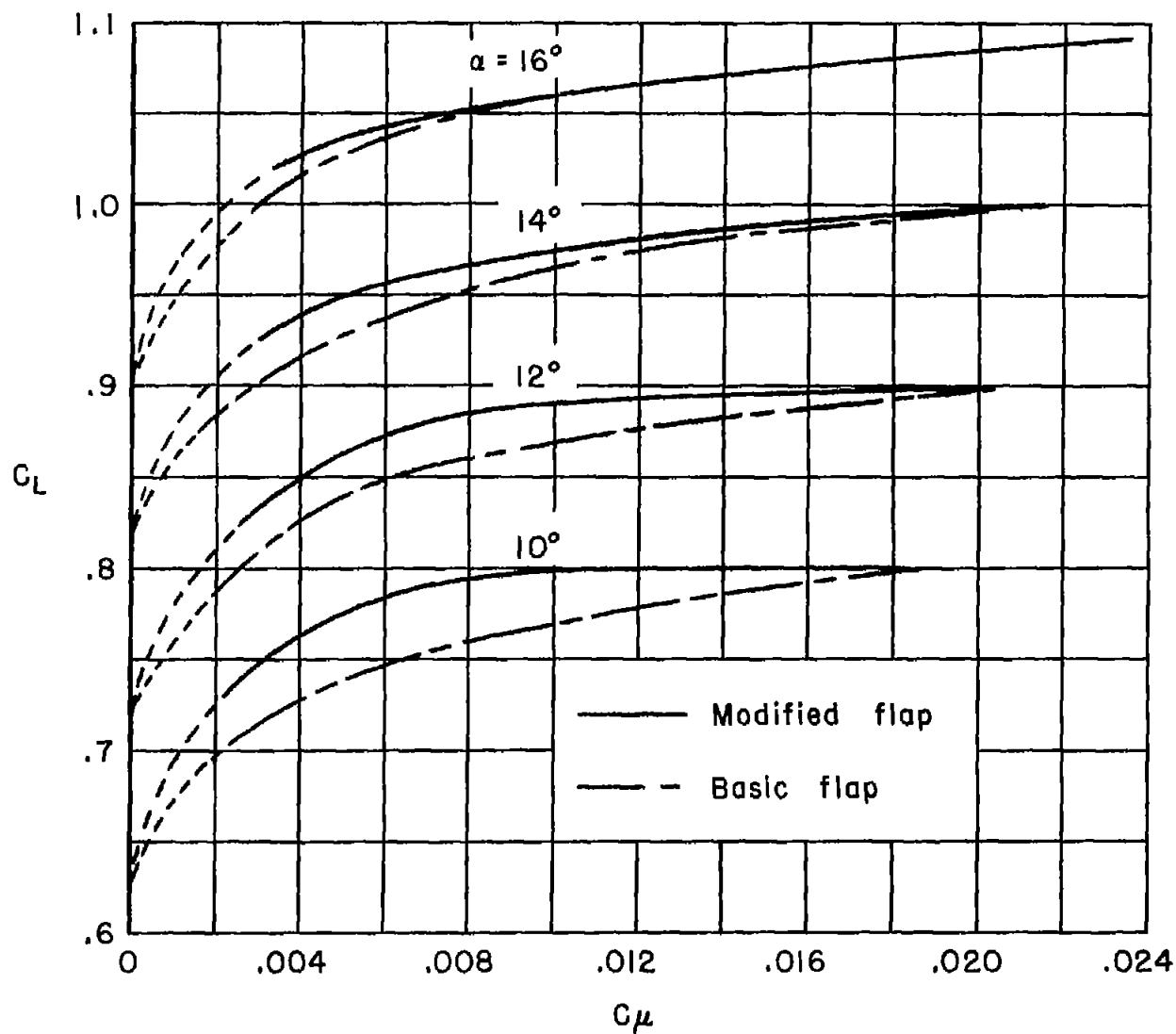


Figure 13.- Variation of lift coefficient with momentum coefficient.

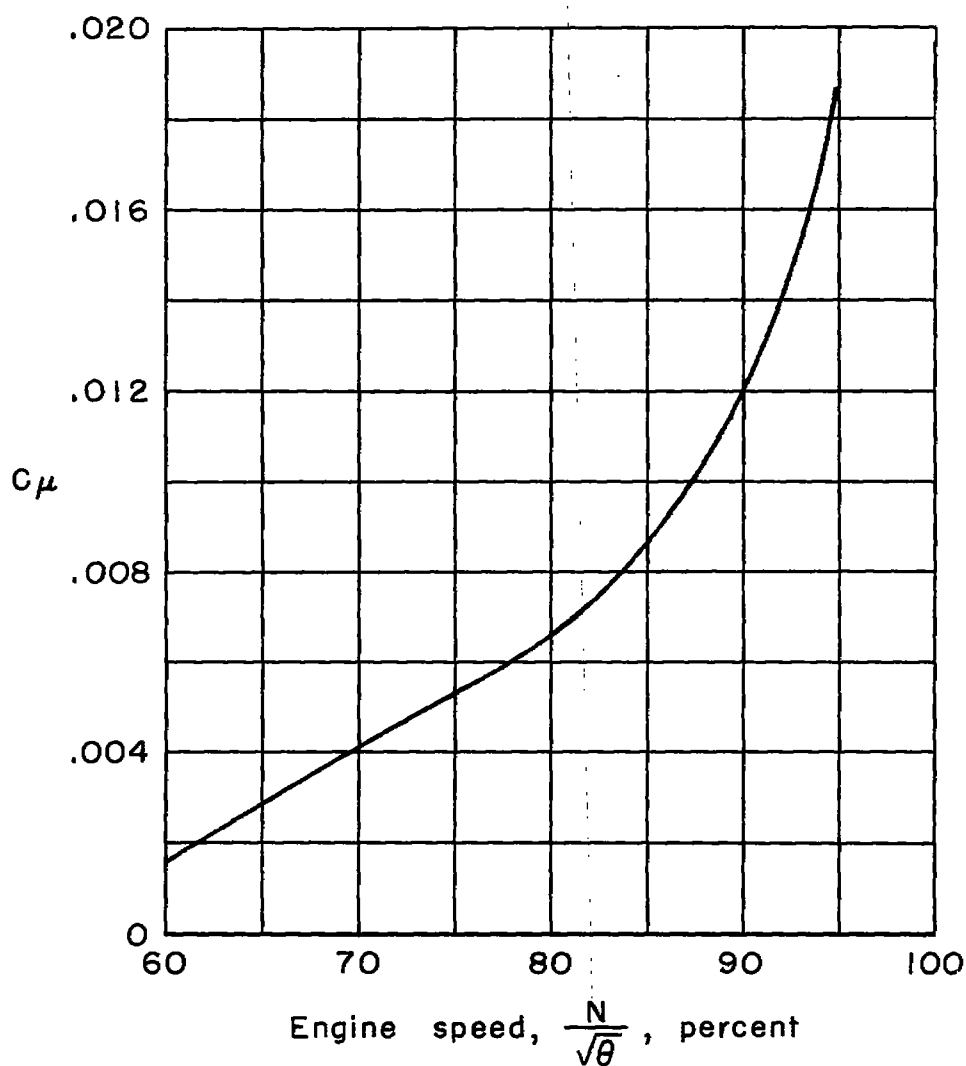


Figure 14.- Variation of momentum coefficient with engine speed;  $C_L = 1.0$ , altitude = 10,000 feet.

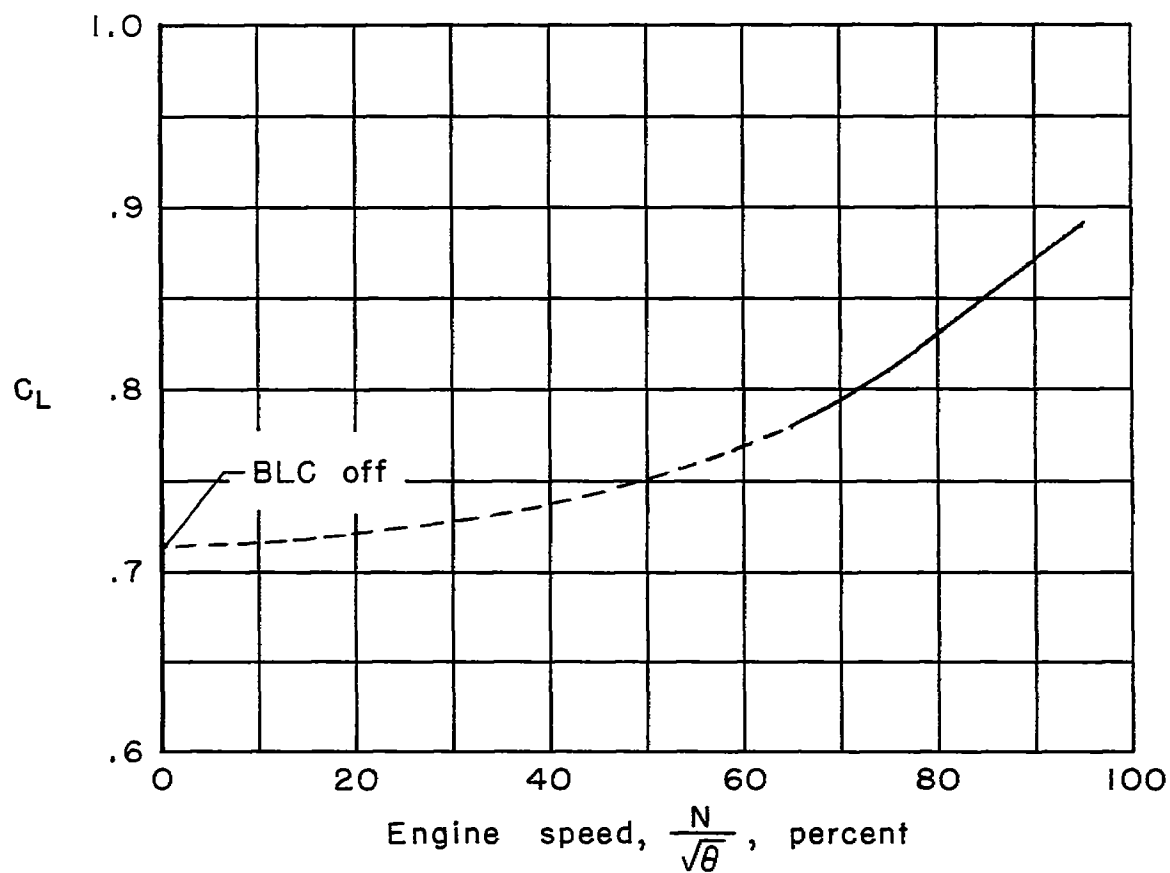


Figure 15.- Effect of engine speed on lift for  $\alpha = 12^\circ$ ;  $\delta_f = 45^\circ$ .

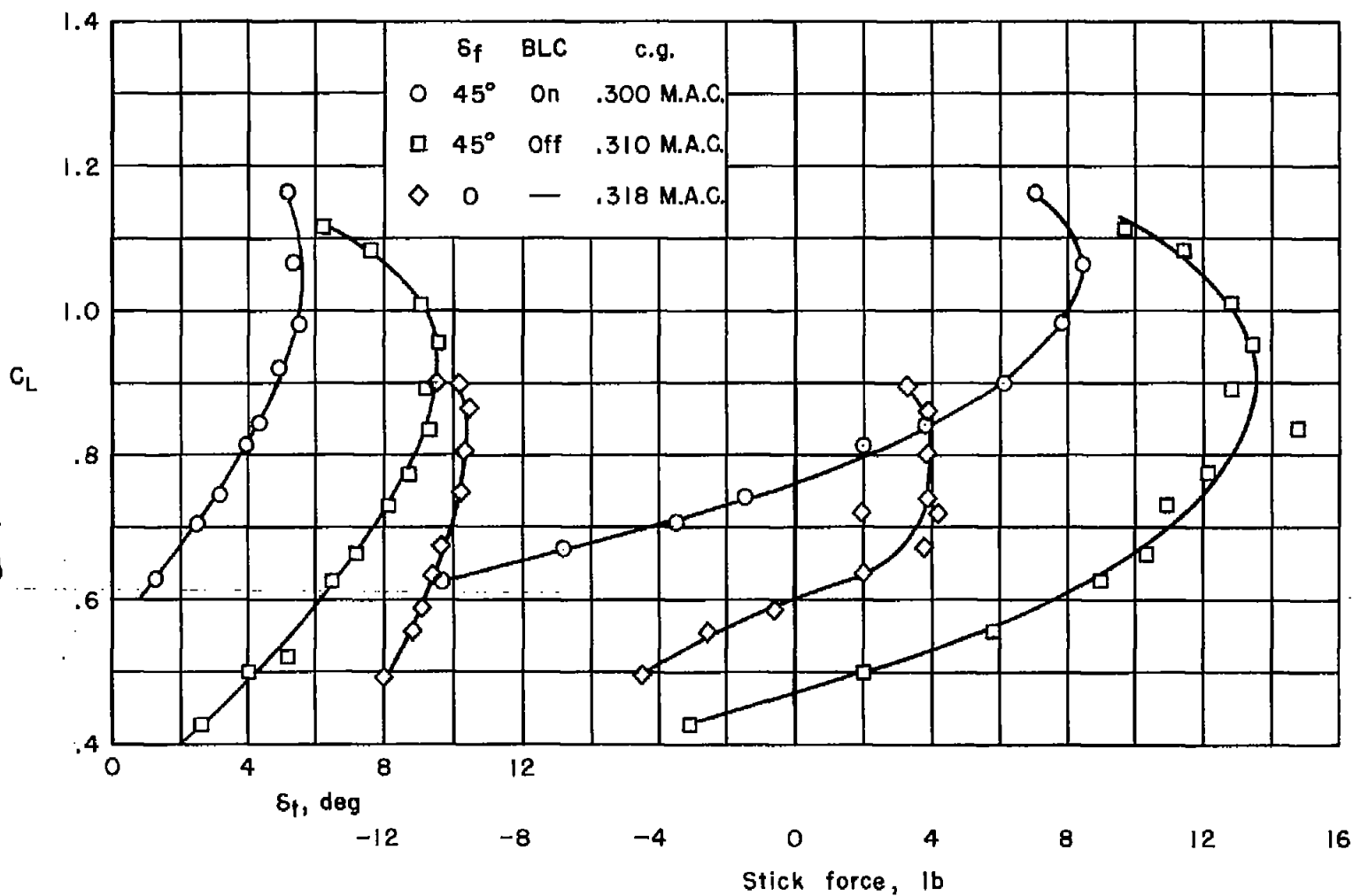


Figure 16.- Static longitudinal stability.

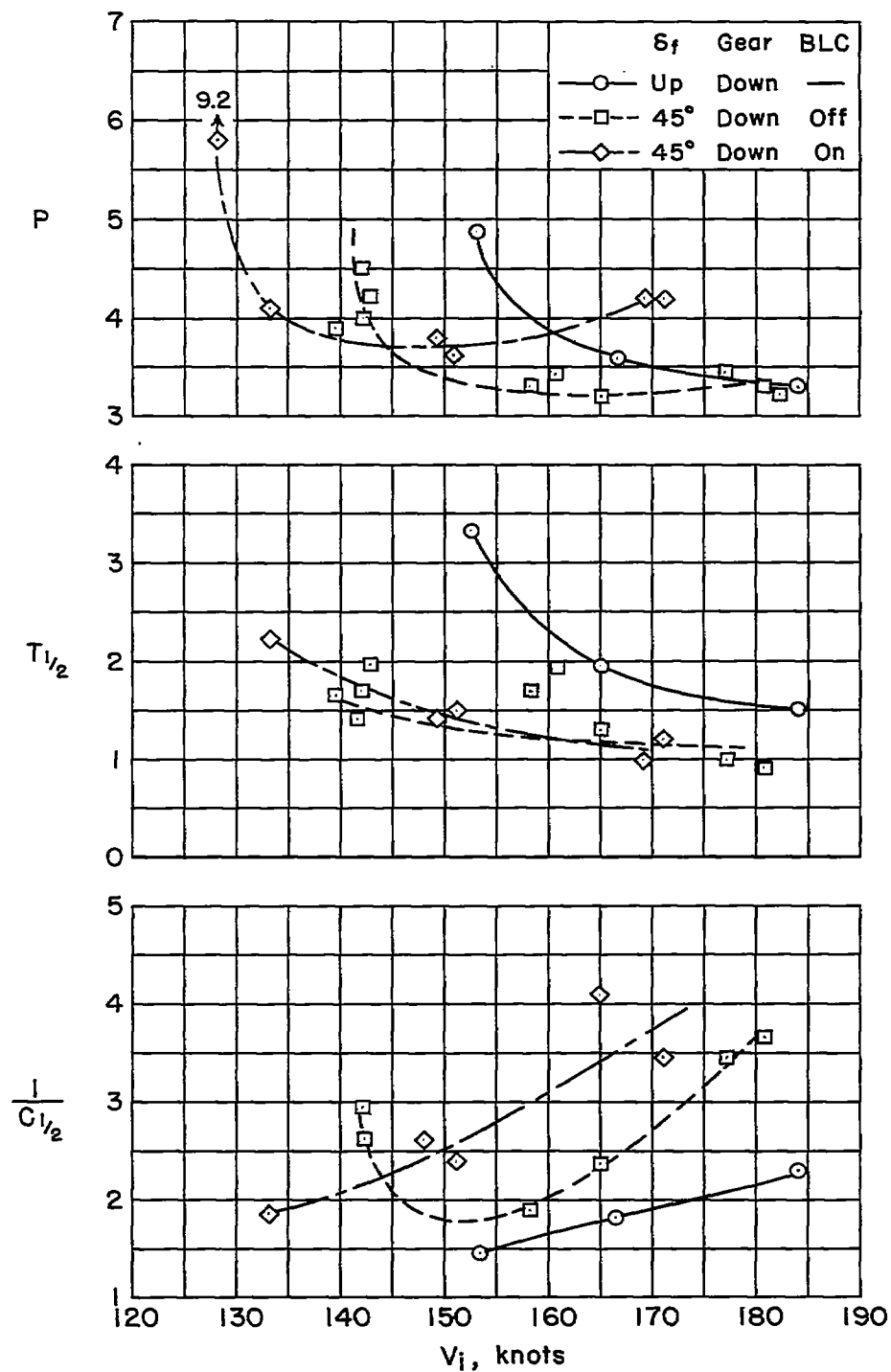


Figure 17.- Dynamic longitudinal stability characteristics.



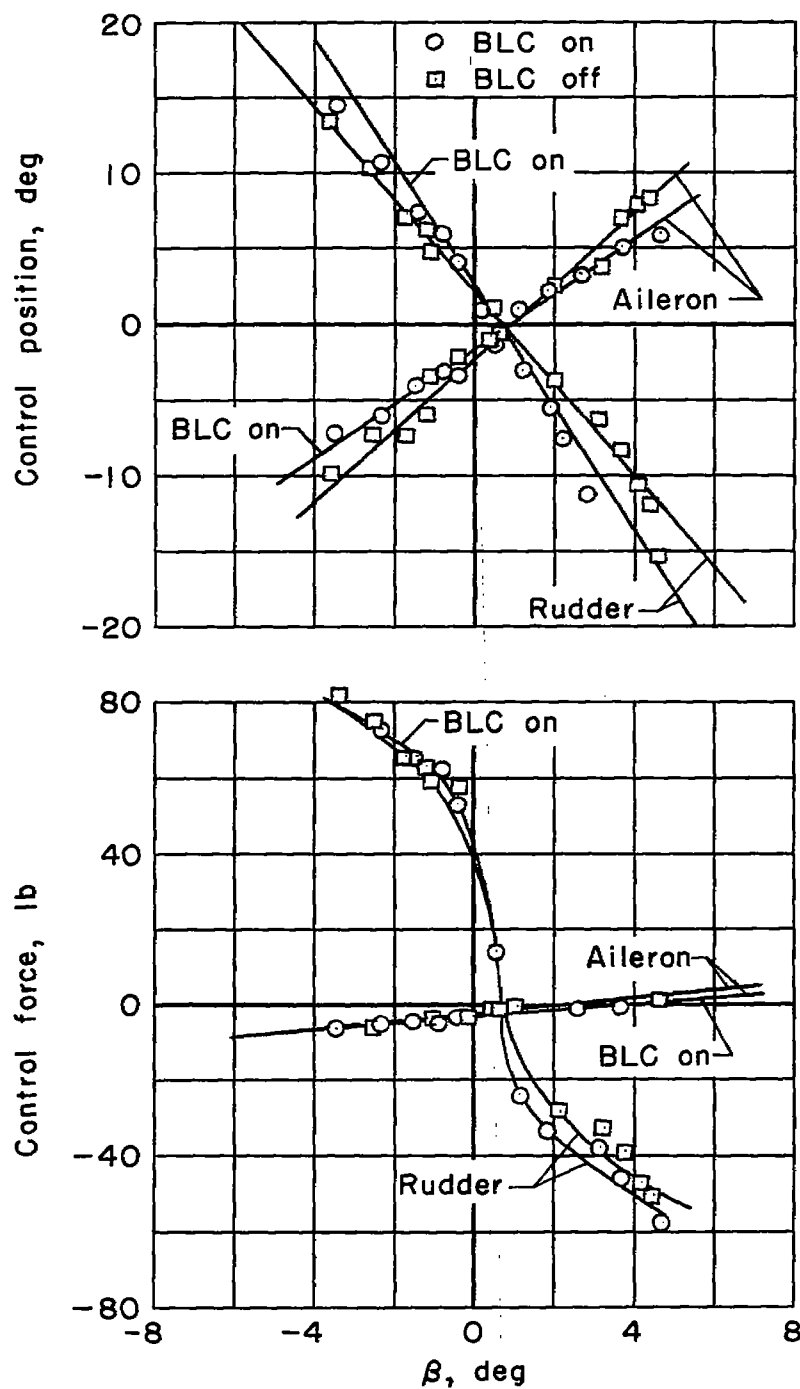


Figure 18.- Aileron and rudder position and force required for steady sideslip;  $\delta_r = 45^\circ$ .

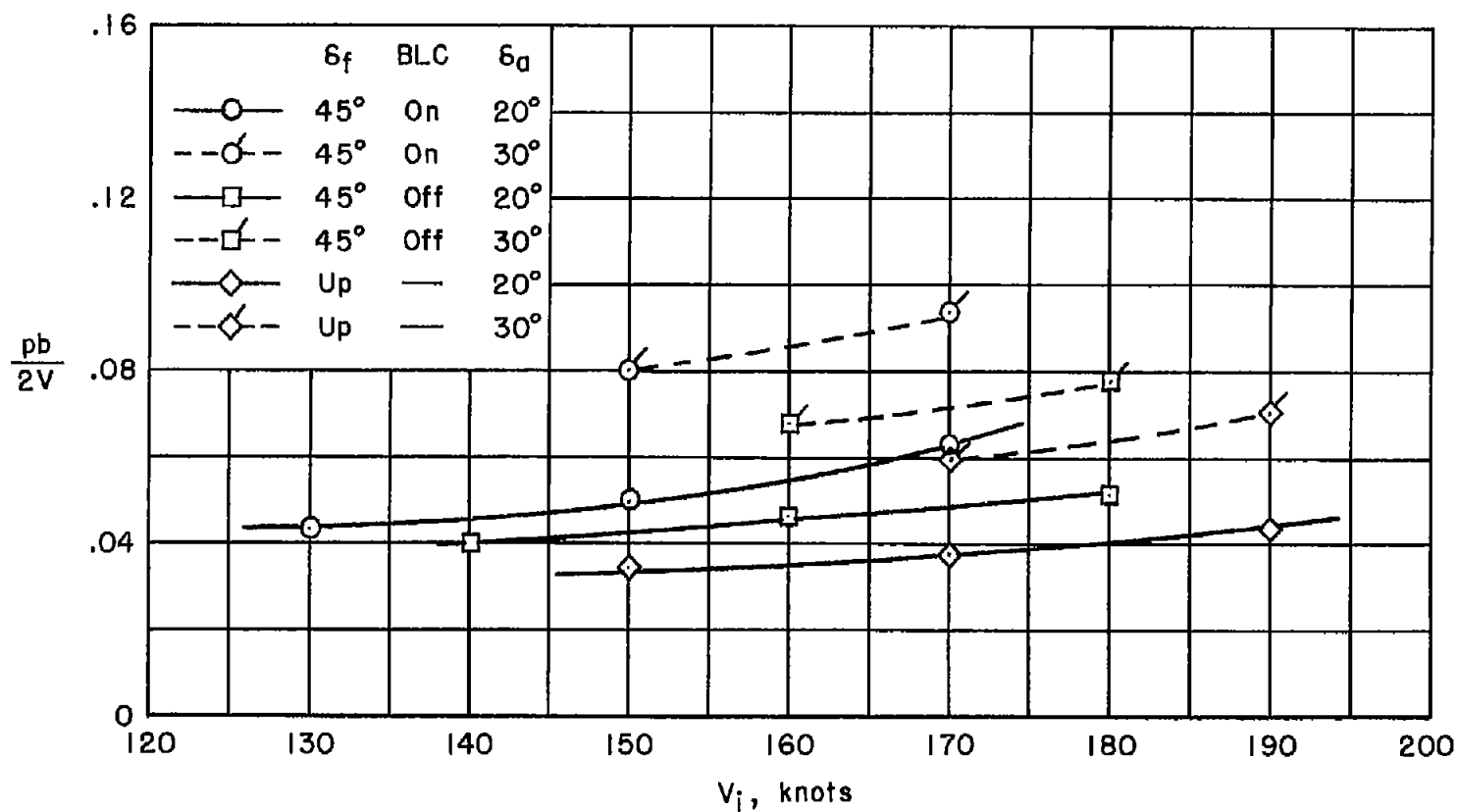
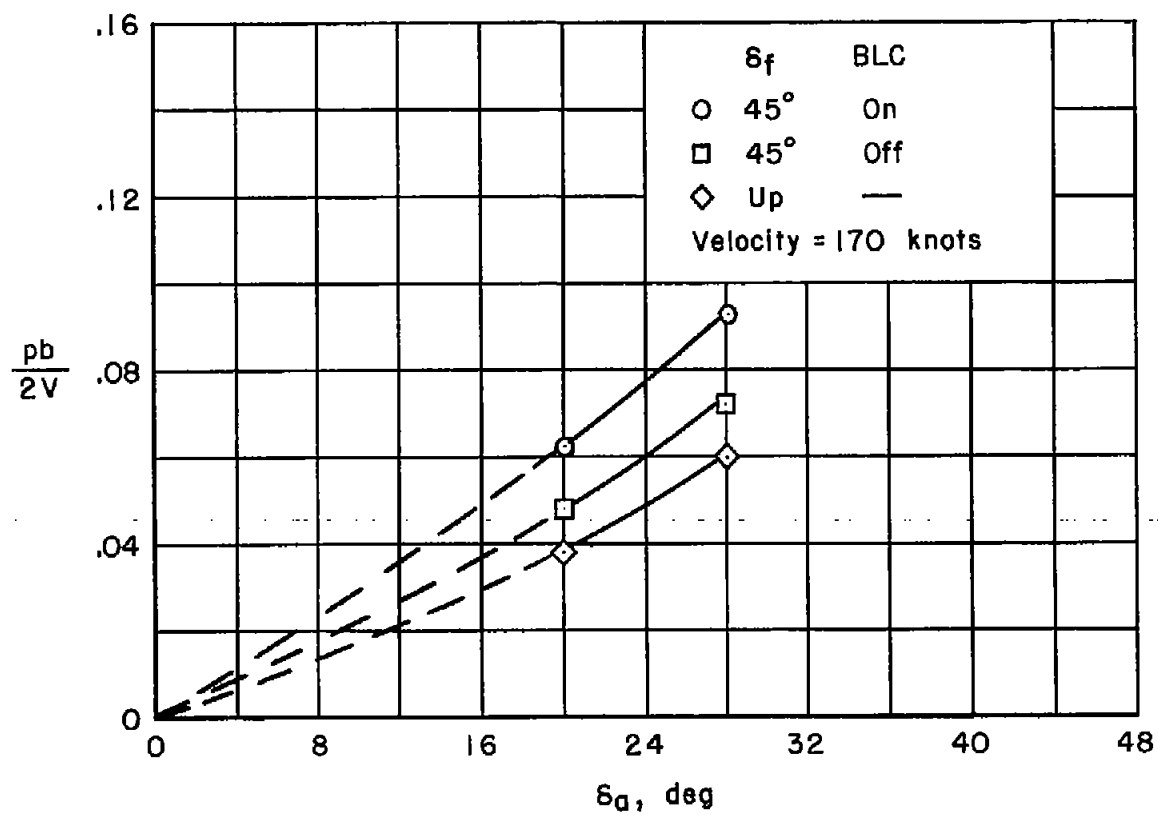
(a) Variation of  $pb/2V$  with airspeed.

Figure 19.- Effect of airspeed and aileron deflection on the rolling performance.



(b) Variation of  $\frac{pb}{2V}$  with aileron deflection.

Figure 19.- Concluded.

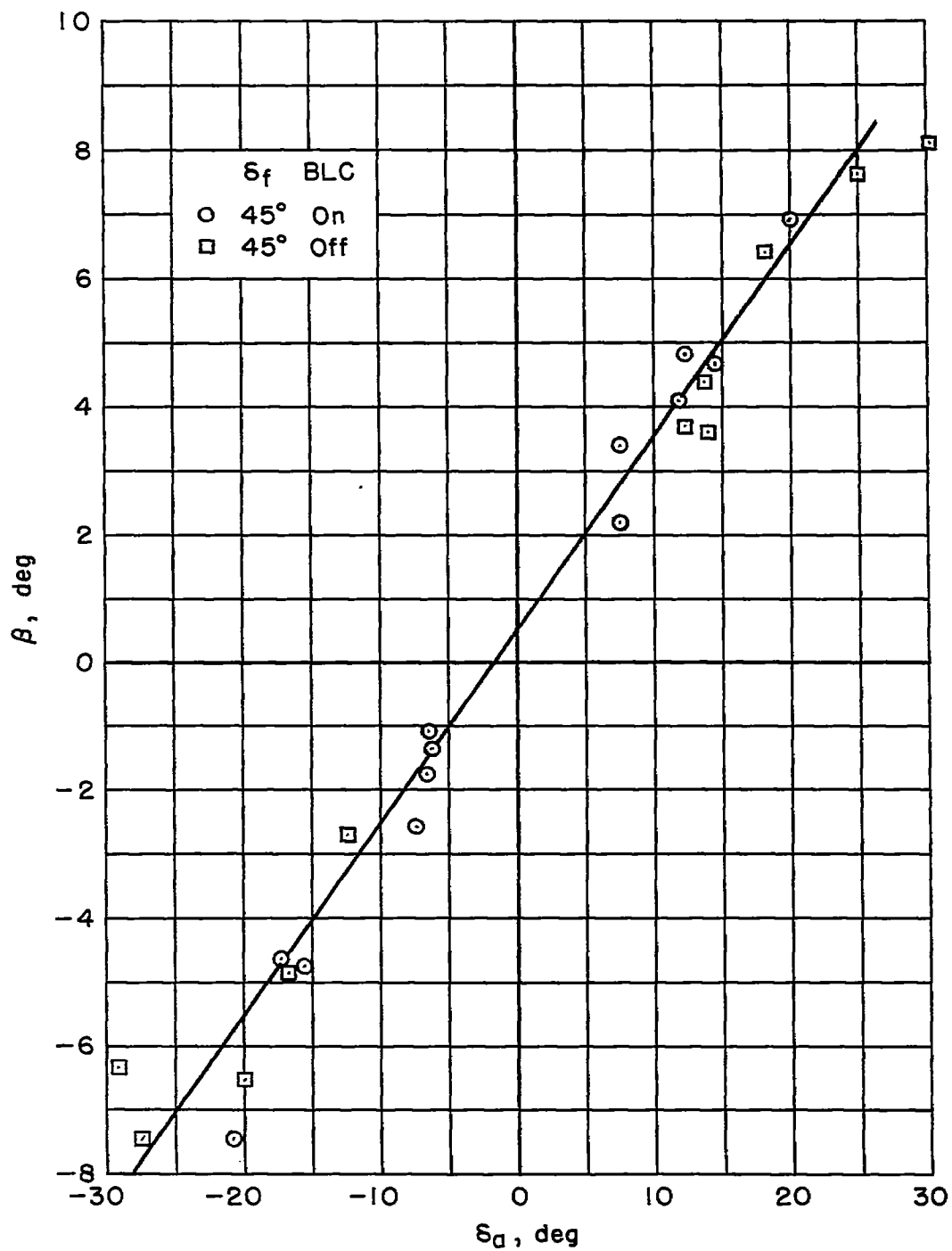
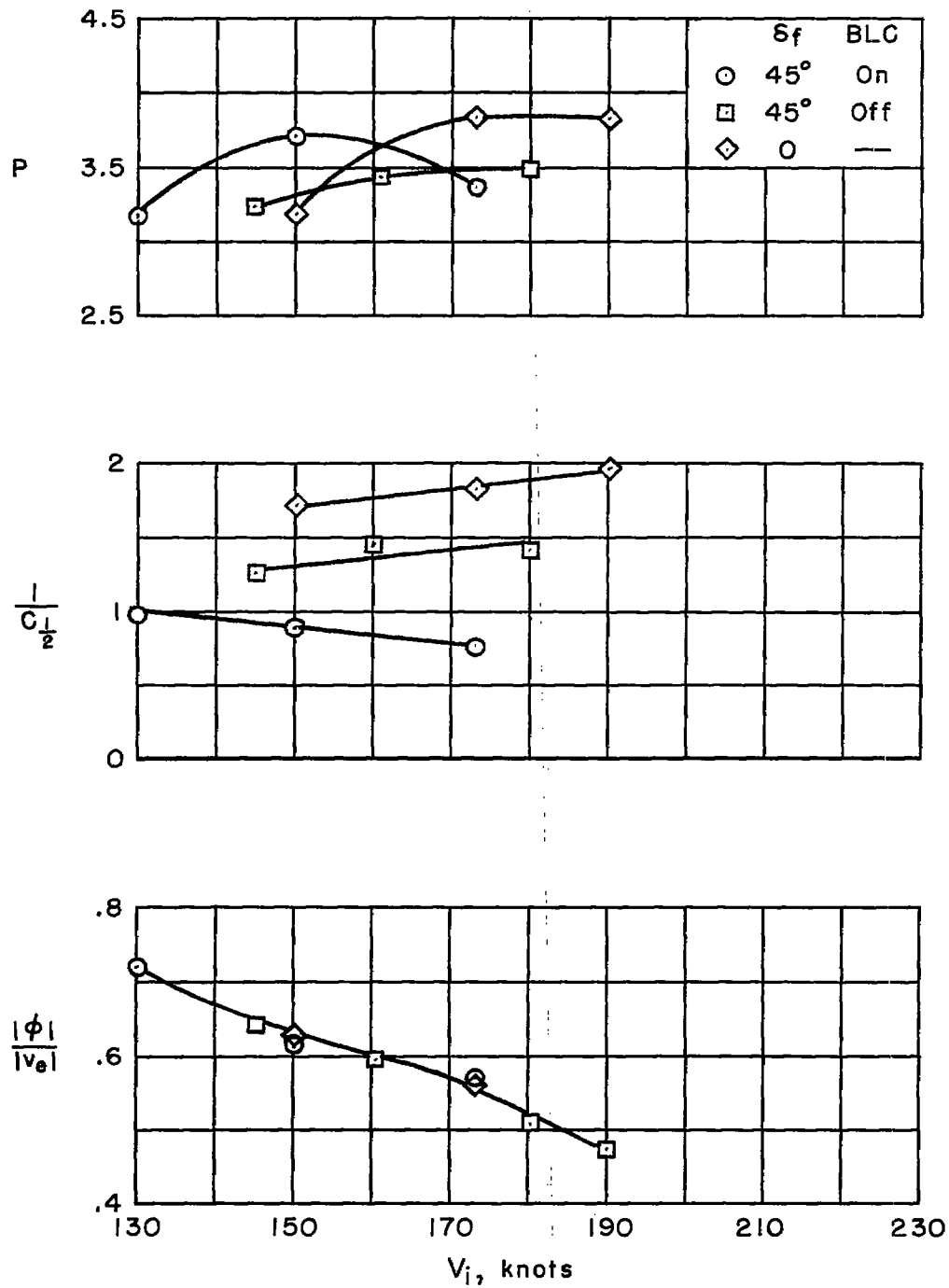
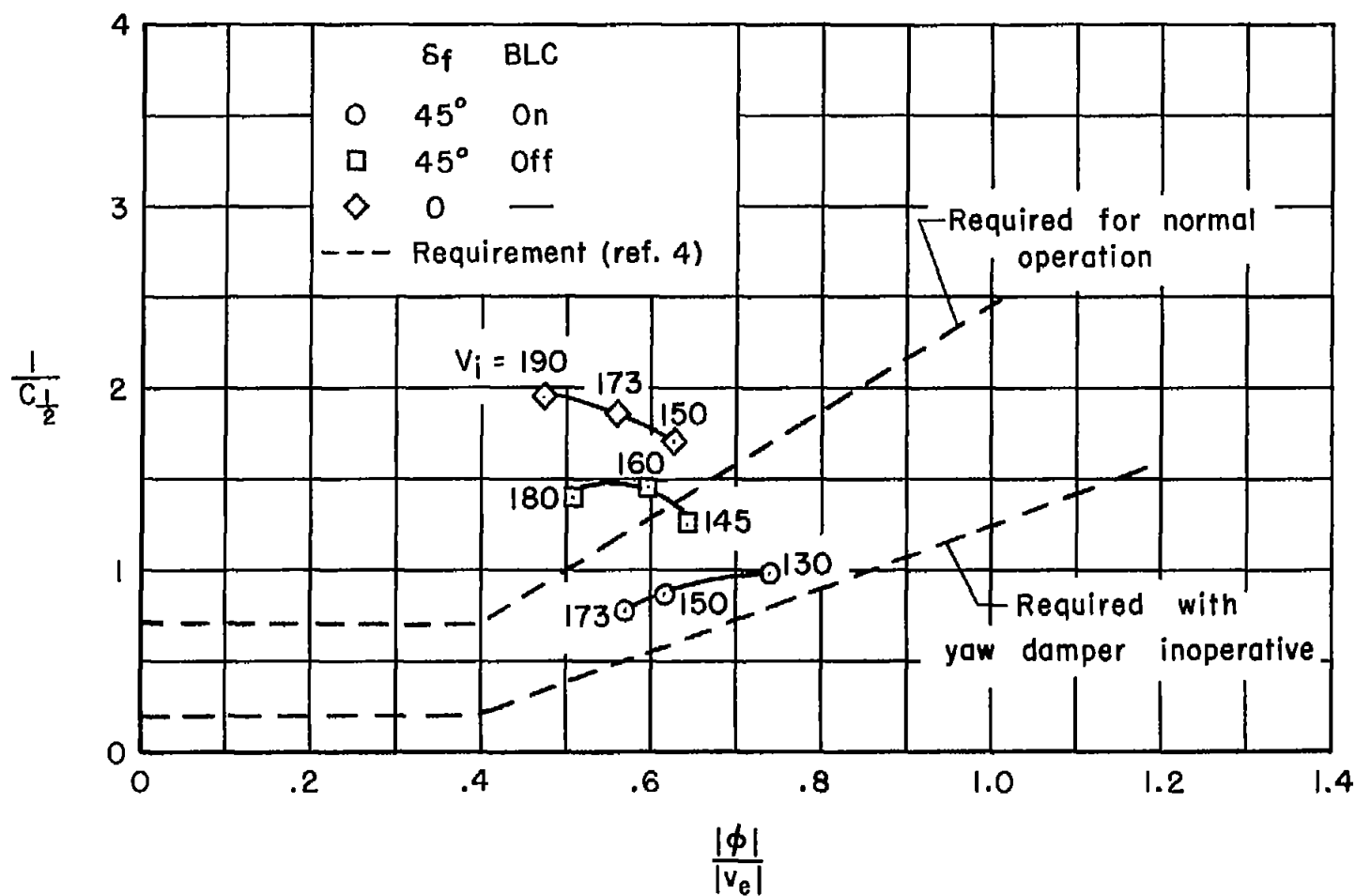


Figure 20.- Variation of adverse yaw with aileron deflection during aileron rolls;  $V \approx 140$  knots.



(a) Variation of period, damping, and rolling parameter with airspeed.

Figure 21.- Lateral oscillatory characteristics.



(b) Variation of the damping parameter with the rolling parameter.

Figure 21.- Concluded.

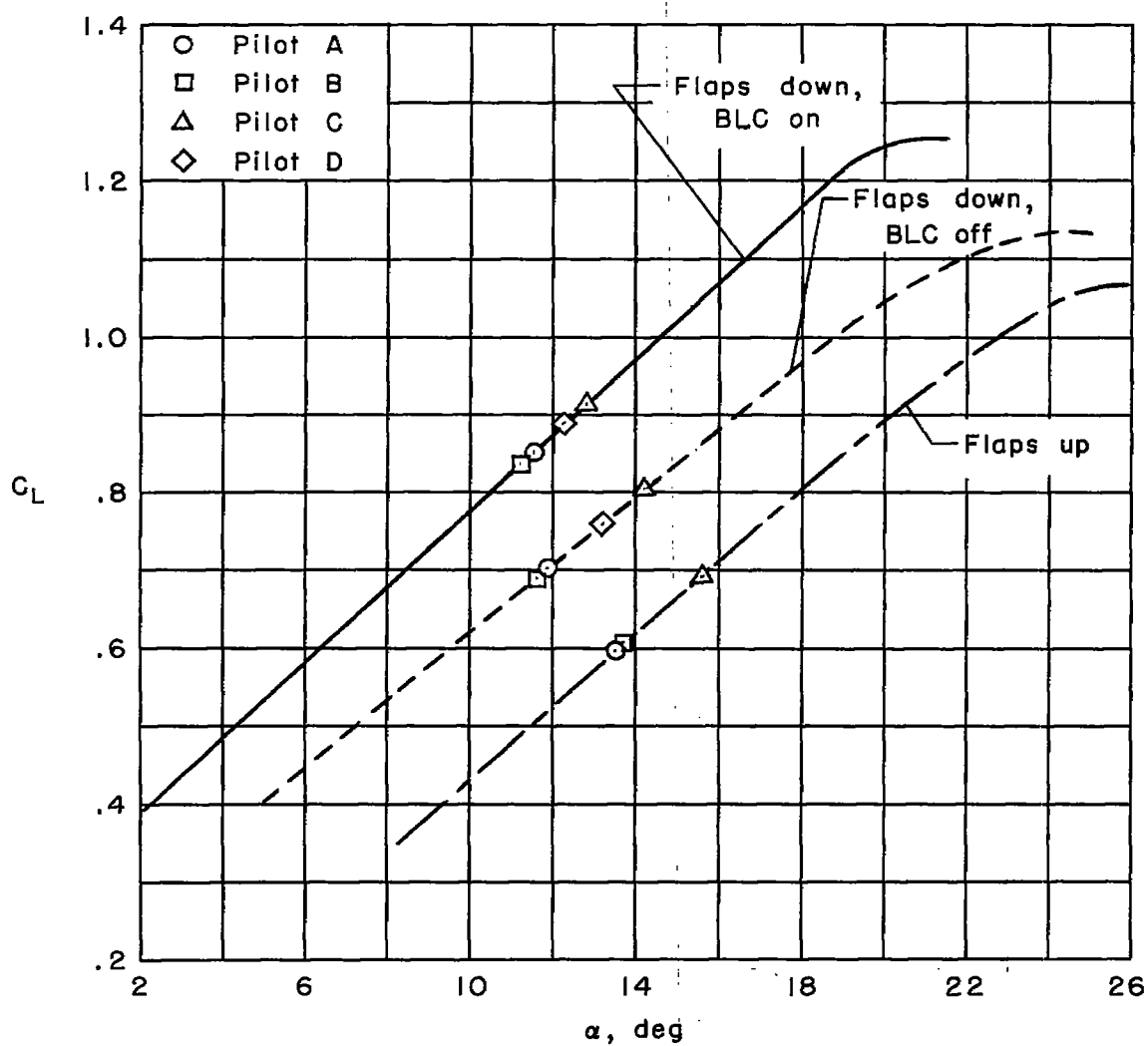


Figure 22.- Variation of lift coefficient with angle of attack;  
gross weight = 22,000 pounds.

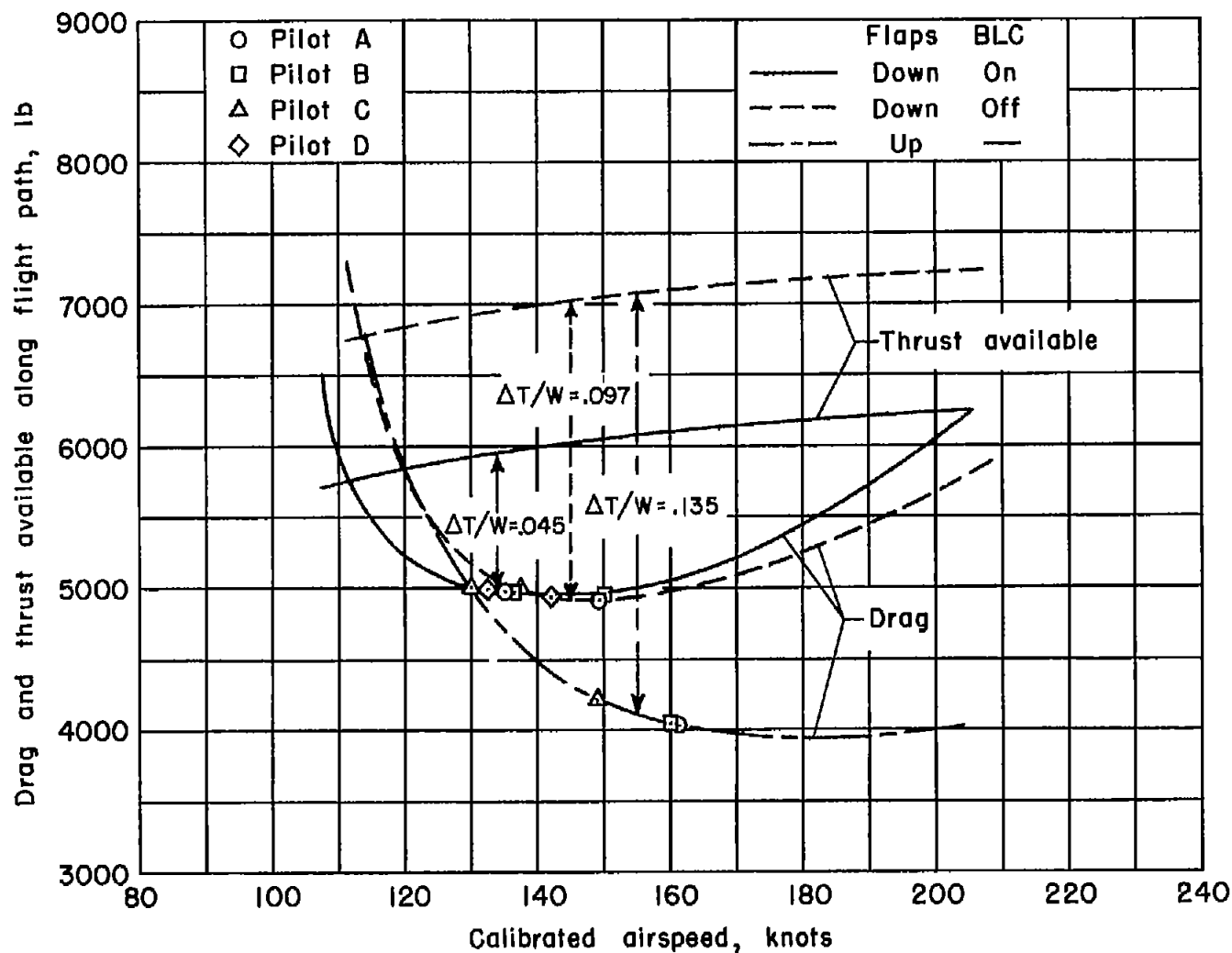


Figure 23.- Variation of drag and thrust available along flight path with calibrated airspeed; pressure altitude = 200 feet, temperature = 75° F, gross weight = 22,000 pounds.



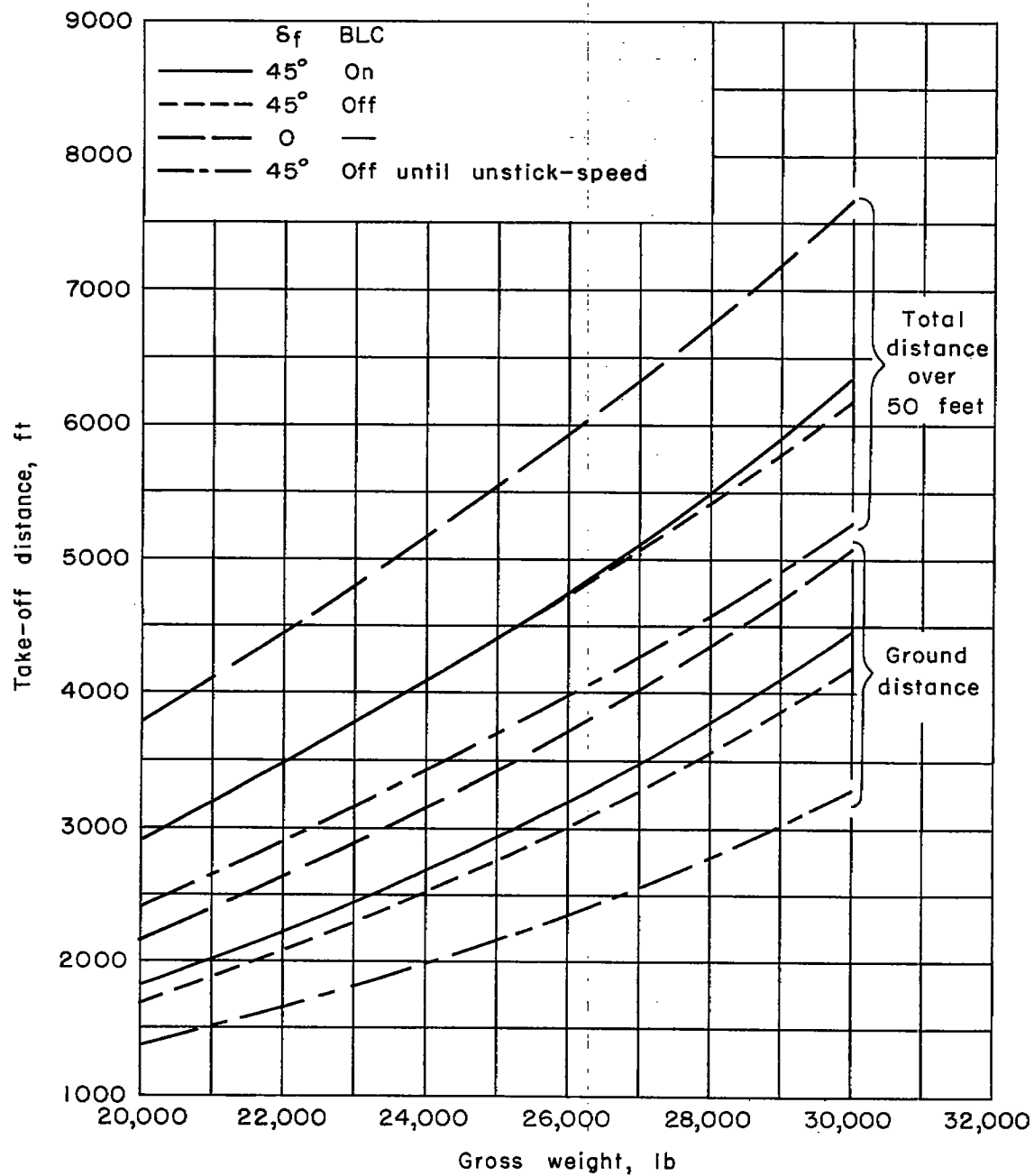


Figure 24.- Variation of computed take-off distance with gross weight.

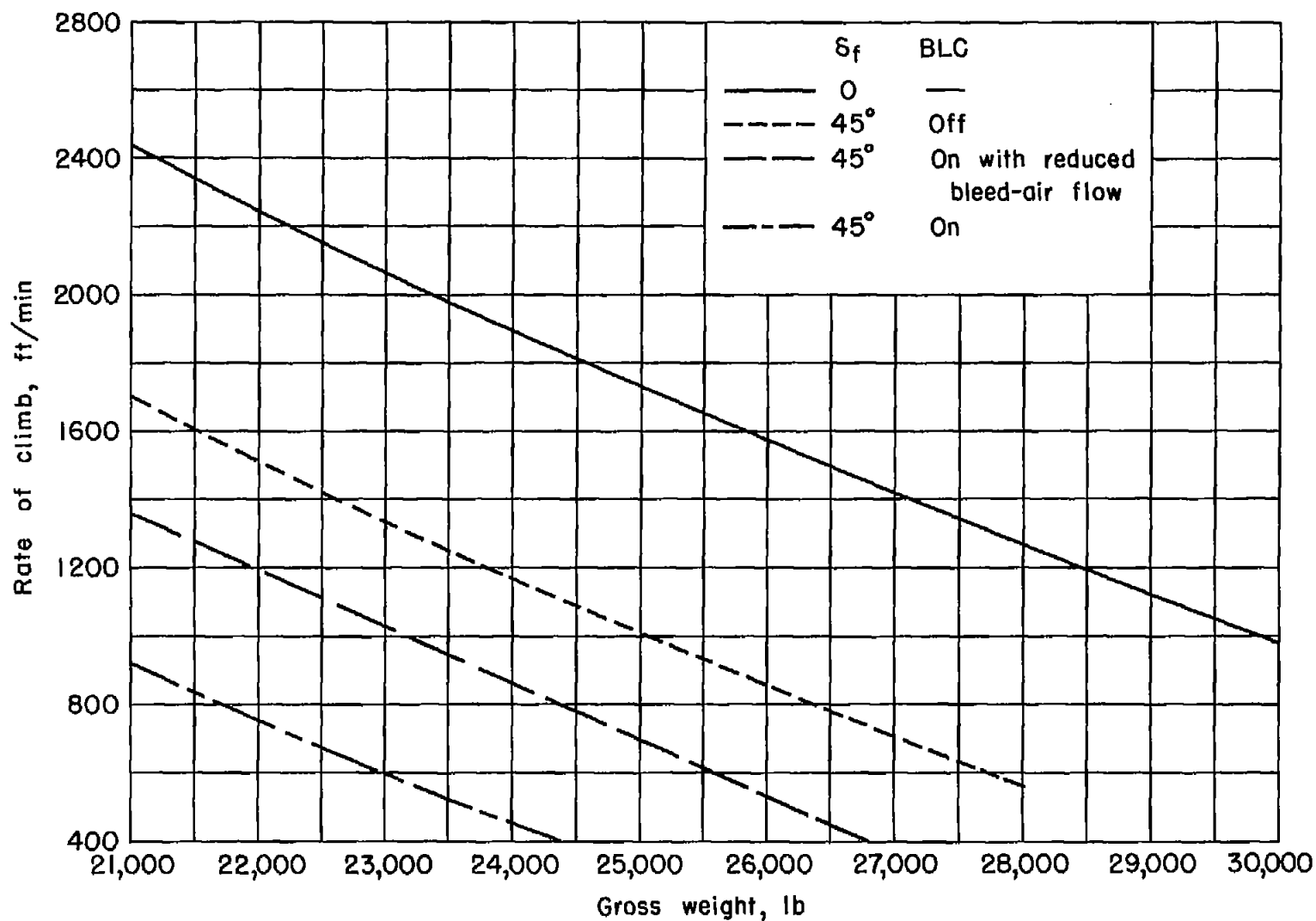


Figure 25.- Variation of computed rate of climb at approach speed with gross weight.

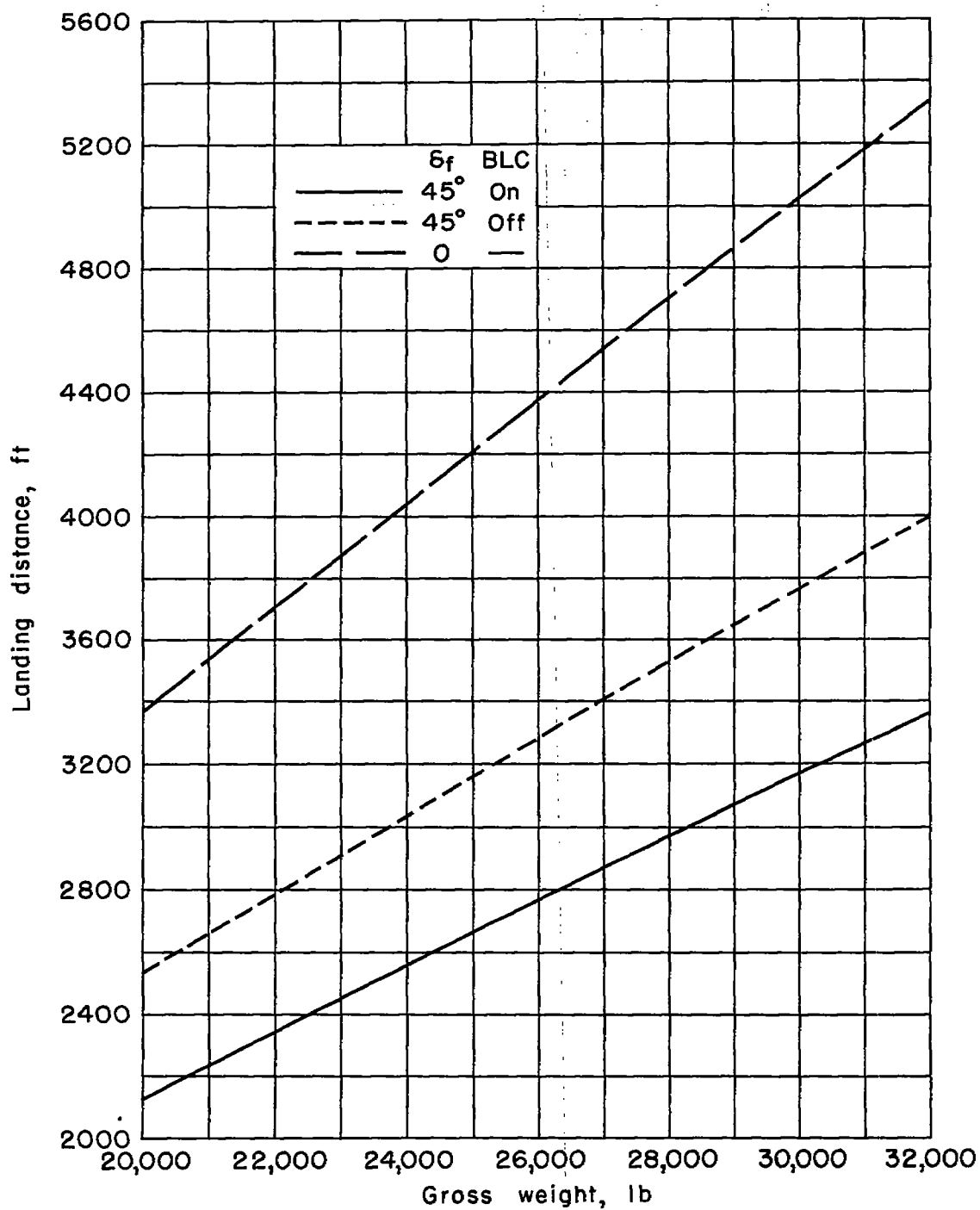


Figure 26.- Variation of computed landing distance with gross weight.